Gilson Paul (Orcid ID: 0000-0001-8778-6795)

Original Research
TRA.12577
doi: 10.1111/TRA.12577
Society number TRA-17-0675
NIH funded NO
Manuscript received 4 October 2017
Revised and accepted 24 April 2018
Sent to press 24 April 2018
Color figures: 1, 2, 3, 4, 5, 6, 7, 8
Supp Mat: 6 figures, 3 tables, 4 movies
Synopsis included YES
Abstract figure included YES
Editorial process file included YES

Spatial organisation of protein export in malaria parasite blood stages.

Sarah C. Charnaud[1#], Thorey K. Jonsdottir[1,2#], Paul R. Sanders[1#], Hayley E. Bullen[1], Benjamin K. Dickerman[1], Betty Kouskousis[1,3], Catherine S. Palmer[1,3], Halina M. Pietrzak[1,2], Annamarrie E. Laumaea[1], Anna-Belen Erazo[1], Emma McHugh[2], Leann Tilley[2], Brendan S. Crabb[1,2,3] and Paul R. Gilson[1,3*].

[1] Burnet Institute, Melbourne, Victoria 3004, Australia.

[2] University of Melbourne, Melbourne, Victoria 3010, Australia

[3] Monash University, Melbourne, Victoria 3800, Australia

# These authors contributed equally.

* Corresponding author

email: paul.gilson@burnet.edu.au

Tel :+61 0433685205

Key words: Malaria, *Plasmodium falciparum*, erythrocyte, protein trafficking, protein export, translocon, PEXEL, PTEX, luciferase.

Synopsis

Malaria parasites export proteins into the human erythrocytes they infect. The exported proteins modify the erythrocyte thereby enabling parasite survival. A protein translocon called PTEX (complex of EXP2, PTEX150 & HSP101), encircles the parasite inside the erythrocyte and knockdown of PTEX appears to arrest protein export. To determine if PTEX directly unfolds and

exports proteins we made reporters that were chemically resistant to unfolding. We found the reporters became bound to PTEX as if lodged in the complex implicating a direct role for PTEX in export. The compound WR99210 binds to exported reporter protein (Hyp1-Nluc-DH) preventing it from being unfolded and resulting in the reporter becoming trapped in the PTEX complex in the parasite. PV, parasitophorous vacuole; ER, endoplasmic reticulum; TVN, tubulo-vesicular network and RBC; red blood cell.

Graphical Table of Contents

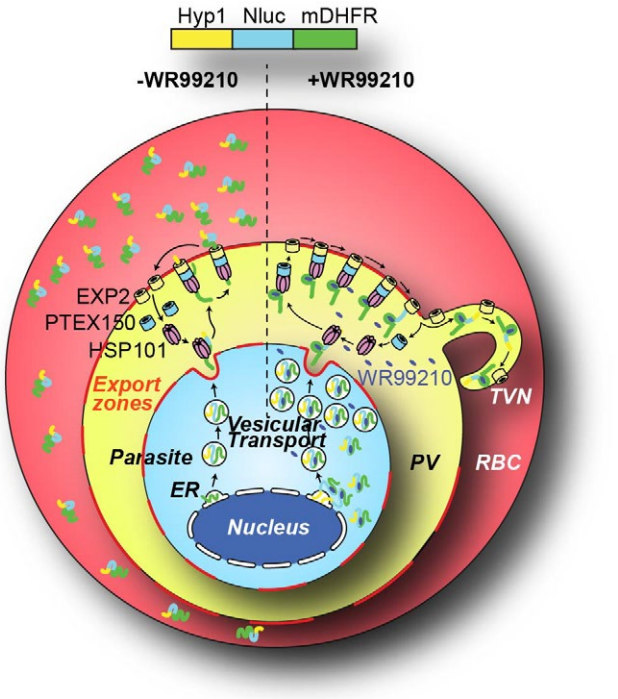

Abstract

Plasmodium falciparum, which causes malaria, extensively remodels its human host cells, particularly erythrocytes. Remodelling is essential for parasite survival by helping to avoid host immunity and assisting in the uptake of plasma nutrients to fuel rapid growth. Host cell renovation is carried out by hundreds of parasite effector proteins that are exported into the erythrocyte across an enveloping parasitophorous vacuole membrane (PVM). The *Plasmodium* translocon for exported proteins (PTEX) is thought to span the PVM and provide a channel that unfolds and extrudes proteins across the PVM into the erythrocyte. We show that exported reporter proteins containing mouse dihydrofolate reductase domains that inducibly resist unfolding become trapped at the parasite surface partly colocalising with PTEX. When cargo is trapped, loop-like extensions appear at the PVM containing both trapped cargo and PTEX protein EXP2, but not additional components HSP101 and PTEX150. Following removal of the block-inducing compound, export of reporter proteins only partly recovers possibly because much of the trapped cargo is spatially segregated in the loop regions away from PTEX. This suggests parasites have the means to isolate unfoldable cargo proteins from PTEX-containing export zones to avert disruption of protein export that would reduce parasite growth.

Introduction

Almost half the world's population are at risk of malaria, the disease caused by infection with *Plasmodium spp.* parasites. In 2015 there was an estimated 212 million cases reported, resulting in 429,000 deaths, mostly of children under 5 [1]. Infection with *P. falciparum* causes the majority of this disease burden, and much of this parasite's pathogenicity can be attributed to its ability to extensively modify the human erythrocyte in which it resides [2]. These modifications are driven by a complement of proteins that are exported into the host cell compartment, that perform many virulence related functions including cytoadherence to the vascular endothelium, nutrient uptake and waste removal [2-4].

To gain access to the host erythrocyte cytoplasm, exported proteins must first be produced in the parasite, trafficked to the parasitophorous vacuole (PV) and then exported across the PV membrane (PVM) into the erythrocyte. A large proportion of the exported proteins identified to date contain a defined export motif termed the Plasmodium Export Element (PEXEL) delineated by the sequence RxLxE/D/Q which is located near the N-terminus of the protein and is specifically cleaved in the ER by the aspartyl protease plasmepsin V [5-9]. By mechanisms not yet understood, plasmepsin V cleavage licenses proteins for traffic to the PV [10] where they are subsequently recognised and extruded across the PVM by the *Plasmodium* Translocon of Exported proteins (PTEX) [2,11,12].

The PTEX complex contains five core protein subunits HSP101, EXP2, PTEX150, TRX2 and PTEX88 [2]. The heat-shock protein HSP101 likely contributes to the unfolding of cargo and supplies energy to the complex through its ATPase function. EXP2 forms oligomers and is associated with the PVM, and is presumed to form a protein translocating pore through the PVM [13,14]. PTEX150 probably serves a structural role acting to link EXP2 and HSP101. All three of these proteins are essential for the survival of *Plasmodium* parasites [2,11-13,15]. TRX2 and PTEX88 are not essential for survival of the rodent malaria parasite *P. berghei,* but are important for efficient protein export and potentially serve auxillary functions such as recognition of protein cargo subsets [11,16,17]. Additional PTEX associated proteins have recently been identified including Pf113, and the exported chaperone HSP70-x [15]. An additional export interacting complex (EPIC) containing parasitophorous vacuole proteins 1 and -2 (PV1 and PV2) is anchored to the PVM via exported protein 3 (EXP3) [18]. These proteins do not represent core components of the PTEX complex and possibly play ancillary roles such as recognising subsets of cargo proteins.

To probe the function of the PTEX complex, conditionally trappable exported cargo molecules have been expressed in parasites and the effects of conditionally trapping and releasing of the cargo has been assessed [19]. Immunoprecipitation assays (IPs) revealed that the trapped cargo associates strongly with PTEX component, EXP2

but not HSP101 [19]. Given that previous studies have shown exported cargo can be co-precipitated with each of the core PTEX components [2,13], we decided to employ a different trappable cargo approach to glean further insights into the process of protein export at the PVM.

Here we have utilised a trappable nanoluciferase (Nluc) reporter construct containing the murine dihydrofolate reductase enzyme (mDHFR) which is refractory to unfolding in the presence of WR99210 (WR) to further probe PTEX function [20]. Nluc reporter proteins are highly quantifiable and have been used previously to examine the export of PEXEL proteins, resistance to sorbitol lysis, merozoite egress and invasion and other aspects of the parasite's life cycle [21-26]. Here, we generated multiple exported constructs containing both Nluc and mDHFR, but with different additional epitope and affinity tags and followed their fates. We show that different constructs do indeed behave differently upon trapping at the PVM with some constructs partially resuming export after WR removal, while others remain completely blocked. We also found that the trapped cargo clusters with PTEX at the parasite surface and co-precipitation indicates direct interaction. Interestingly some trapped cargo also localises to membranous loops extending from the PVM containing only EXP2 and not the other PTEX components.

Results

Exported nanoluciferase-murine dihydrofolate reductase reporter proteins can be expressed in P. falciparum.

To generate conditionally trappable reporter constructs, we utilised an exported Nluc construct containing the first 113 amino acids of the exported PEXEL protein Hyp1 (PF3D7_0113300) appended to the N-terminus of the Nluc sequence (Figure 1A) [21]. Proteins containing mDHFR become highly resistant to cellular unfolding mechanisms when bound to the antifolate ligand WR99210 (WR), and their blockage at the PV/PVM has previously been demonstrated through the use of exported GFP-mDHFR reporter strains [19,20,27,28]. At the C-terminus of this construct we inserted the sequence for mDHFR to produce the fusion construct Nluc-DH (Figure 1A, top).

Two additional constructs were made by appending different reporter elements to the Nluc-DH construct. The first included an engineered ascorbate peroxidase (APEX) that catalyzes the H_2O_2-dependent polymerization of diaminobenzidine to provide contrast for imaging by transmission electron microscopy [29] (Nluc-DH-APEX) (Figure 1A, middle). The other reporter contained a Halotag (Halo) that is an engineered bacterial hydrolase that covalently attaches itself to a chloroalkane moiety [30] and can therefore be used for imaging and pull-down assays (Figure 1A, bottom, Nluc-DH-Halo). We included both APEX and Halotag reporters in our analyses so that the location of trapped cargo could be imaged at high resolution by electron and super-resolution microscopy, respectively. A TY1 epitope tag was also inserted near the C-terminus of Nluc-DH-APEX to facilitate the isolation of the reporter protein with a specific antibody (Figure. 1A).

The Nluc-DH, Nluc-DH-APEX and Nluc-DH-Halo fusion sequences were inserted into the pEF plasmid under control of the *P. berghei* EF1α promoter that had its human DHFR gene replaced with blasticidin deaminase [21]. Reporter constructs were transfected into the *P. falciparum* CS2 strain previously transfected with a construct appending an haemagglutinin (HA)-epitope tag and a *glmS* ribozyme to the C-terminus of the endogenous *ptex150* gene [11]. Since this parasite strain was resistant to WR treatment, the drug could be utilized to block export of our reporter proteins without having additional deleterious effects on the parasite.

To verify expression of these constructs western blots of the parasites lines treated +/- 10 nM WR were probed with anti-Nluc IgG, which detected bands close to the predicted sizes of 51 kDa (Nluc-DH), 78 kDa (Nluc-DH-APEX), and 85 kDa (Nluc-DH-Halo) (Figure 1B). Concentrations of WR from 0.15 to 10 nM were determined to not substantially reduce parasite growth in a single intraerythrocytic cell cycle from ring stage to trophozoite stage (Figure S1A). Lactate dehydrogenase activity based growth assays also

indicated no growth reduction following WR treatment for a whole 48 h cell cycle (Figure S1B). The western blot data confirmed that 14-18 h treatment +/- 10 nM WR did not impact expression of the reporter constructs since the Nluc signal +/- WR were similar. Furthermore, these data suggest that 14-18 h treatment +/- WR was not deleterious to the parasites as expression levels of endogenous EXP2 and PfHSP70-1 was the same (Figure 1B). Furthermore, levels of the late-ring expressed exported GBP130 protein were very similar in all lines indicating no WR-dependent delay in progression though the intraerythrocytic cell cycle (Figure 1B). In Nluc-DH-APEX the same ~75 kDa band was also detected with a mouse anti-TY1 monoclonal antibody (Figure S2).

The export of nanoluciferase-murine dihydrofolate reductase reporter proteins can be blocked in a WR dependent manner.

Next we quantified the WR-induced trapping of mDHFR containing PEXEL fusion proteins across the whole parasite population. To do this we employed export assays used previously in which the parasites were differentially permeabilised to measure the contents of either the erythrocyte (exported), the PV or the parasite compartment [19,20,27,28]. Briefly, proteins exported into the erythrocyte compartment (RBC) of trophozoite stage Nluc-DH-Halo parasites were released with equinatoxin II which permeabilised the erythrocyte membrane (Figure 2A,B) [31]. Proteins resident or trapped in the PV as well as the erythrocyte compartment were released by treatment with saponin and all cell compartments were permeabilised with Triton X-100 (Figure 2A,B). To validate membrane permeabilisation the parasites were treated +/- proteinase K to degrade the exposed proteins no longer protected by membranes. After separating soluble and insoluble cellular components (pellet) the proteins were fractionated by SDS-PAGE and detected by western blot. The experiment indicated that the PEXEL protein, GBP130, was mostly exported as a soluble protein into the erythrocyte (RBC) compartment where it could be digested by proteinase K after equinatoxin treatment (Figure 2A). EXP2 as expected was an insoluble PV protein susceptible to proteinase K digestion after saponin treatment. The Nluc-DH-Halo protein appeared to mostly segregate between the erythrocyte and PV compartments with lesser amounts with in the parasite (Figure 2A). Pre-treatment with 10 nM WR for 16 h did not appear to strongly alter the proportions of Nluc-DH-Halo exported into the erythrocyte versus trapped in the PV but we note that signal levels often varied greatly from lane to lane making it difficult draw conclusions.

With the western blot approach not well suited to quantify subtle changes in protein export efficiency we decided to exploit the bioluminescence properties of our reporter proteins (Figure 2B,C). Since bioluminescence is highly sensitive and quantitative the export assays were miniaturised into a microplate format enabling more WR concentrations to be evaluated. We used the differential permeabilisation methods described above to release the Nluc reporters from their various compartments. The bioluminescence signal was produced when Nluc reporters gained access to their NanoGlo substrate in the surrounding buffer (Figure 2B). In the absence of WR, >90% of Nluc-DH, Nluc-DH-APEX and Nluc-DH-Halo fusion proteins were exported into the erythrocyte compartment of trophozoite stage parasites (Figure 2C). The remaining fusion protein was split between the PV and parasite compartments. In control PTEX150-HA parasites expressing an exported Nluc protein lacking a DH domain about 90% of the Nluc protein was also exported in the absence of WR (Figure 2C).

To quantify WR induced trapping, ring stage parasites were cultured in a titration series of WR concentrations for 16 h and when trophozoites the export assay was performed. As anticipated there was a WR dependent reduction in export in the parasite lines with Nluc-DH and Nluc-DH-Halo requiring 10 nM WR to block about 50% of the export signal. Trapping of the Nluc-DH-APEX reporter protein was even more dramatic, with almost maximal inhibition with just 2.5 nM WR (Figure 2C). Concentrations of WR higher than 10 nM were not evaluated to determine if export blocking could be increased. Since 50% inhibition of export was sufficient for our work 10 nM WR was used for all subsequent experiments. In the Nluc control parasites the export of the reporter protein was not reduced by WR (Figure 2C). Surprisingly, all WR-trapped Nluc-DH fusion

proteins appeared to accumulate in the parasite cytoplasm, as well as in the PV (Figure 2C).

WR induced blockage of Nluc-DH fusion protein export caused the reporters to become trapped in the PV and the parasite.

To confirm the results of the export assay we performed immunofluorescence (IFA) microscopy on parasites expressing the various reporter proteins. Nluc-DH and Nluc-DH-APEX parasites were colabelled with antibodies to Nluc and EXP2 to distinguish the PV compartment from the parasite and the erythrocyte cytoplasms. Concordant with the export assay indicating the Nluc reporters were efficiently exported without WR, Nluc labelling was most notably detected in the erythrocyte cytoplasm (Figure. 3A,B).

To investigate where treatment with WR blocks the reporter proteins during their trafficking to the erythrocyte cytoplasm, we treated Nluc-DH and Nluc-DH-APEX ring stage parasites for 16 h with 10 nM WR and then performed IFAs when the parasites were trophozoites. These analyses demonstrate that in the presence of WR, the reporter proteins were restricted to the parasite circumference probably at the PV and likely near the PTEX complex, as evidenced by their colocalisation with EXP2 and PTEX150 (Figure 3A, B).

To assess export in the Nluc-DH-Halo parasites, live trophozoites were labelled with Oregon green Halotag dye before fixation and probing for EXP2. Consistent with the Nluc-DH and Nluc-DH-APEX parasites, the Halotag fusion protein was efficiently exported (Figure 3C). After treatment with WR, the Nluc-DH-Halo fusion protein was also blocked at the PV, colocalising with EXP2 (Figure 3C).

Interestingly, in WR-treated trophozoites EXP2 often labelled loop structures attached to the PVM that were also partly labelled for all the Nluc-DH reporters (Figure 3A-C, white arrows). To determine if these loops contained the PTEX150, Nluc-DH and Nluc-DH-Halo trophozoites were probed with anti-HA IgG to detect PTEX150-HA and this indicated its near absence from the loops (Figure 3A, C).

The export assay indicated that in addition to an increase in PV signal following WR trapping of the reporter proteins there was almost as much trapping within the parasite (Figure 2C). Microscopy of the WR-treated parasites detected some perinuclear labelling as well as other features indicative of the endoplasmic reticulum and secretory structures (Figure 3D). We note that similar Nluc localisations were also sometimes observed in untreated parasites albeit not as strongly labelled indicating that WR enhances trapping within the secretory system.

We also attempted transmission electron microscopy on diaminobenzidine treated Nluc-DH-APEX parasites to visualize the APEX tag of the trapped cargo proteins at high resolution. Unfortunately, regions of high contrast corresponding to trapped APEX cargo were not clearly discernible at the parasite surface possibly because the expression of the fusion protein was too low (Figure S3). Electron microscopy did however reveal in WR-treated cells various membranous structures extending from the parasite surface that could correspond to the loops observed by fluorescence microscopy (Figure S3).

Super resolution microscopy indicates that WR-blocked exported proteins colocalise with PTEX at the parasite surface.

For improved resolution of the WR-trapped Nluc-DH fusion protein with EXP2 we used structured illumination microscopy (SIM), which increases the volume resolution compared with conventional microscopy by eight-fold [32]. The WR-trapped Nluc-DH fusion protein sometimes adopted the appearance of a 'necklace of beads' around the periphery of the parasite, and frequently showed colocalisation with similarly sized EXP2 'beads' at the PVM (Figure 4A, top). In other cells the profile of labelling of both proteins at the PV was more uniform (Figure 4B, top). Maximum projections of serial optical sections through the cells (Figure 4A, B, bottom) and 3D rotations indicate WR-trapped Nluc-DH and EXP2 colocalised as a patchwork of irregular surface structures at the PV (Videos S1 and S2). As with the previous widefield imaging, EXP2 and WR-trapped Nluc-DH frequently formed strongly labelled 'bubble-like' loops emanating from the PVM (Figure. 4A, B, white arrows).

The Nluc-DH trophozoites were also probed for PTEX150 where it colocalised with the WR-trapped Nluc-DH protein as punctate structures at the PV (Figure 4C, D and videos S3 and S4). As seen in the widefield images, PTEX150 was almost completely excluded from the surface loops containing the trapped Nluc-DH. Since both EXP2 and PTEX150 localised with Nluc-DH at the punctate PV structures, we assume these regions enriched for PTEX to which the fusion protein has been trafficked for export.

We next probed for HSP101, another component of PTEX. Our rabbit anti-HSP101 IgG labelled the PV and not the loops but also labelled the cytoplasm of the parasites (Figure S4A). Unsure if this was specific or not, we probed HSP101-HA parasites that were not transfected with Nluc reporter constructs with a HA monoclonal [2]. SIM images clearly showed HSP101-HA co-labels the PV with EXP2 (Figure 4E, Top). Large EXP2 loops were rarely observed in the HSP101-HA parasites but small EXP2 loop 'buds' were common and did not label for HSP101 (Figure 4E, Bottom and 4F). HSP101 labelling was therefore most similar to PTEX150 with one exception, which was that some HSP101 labelling within the parasite particularly around the nucleus was also observed (Figure 4F).

To determine whether the loops contained parasite cytoplasm or were likely extensions of the PVM, immunofluorescence was performed for the soluble cytoplasmic HSP70-1 protein. Anti-HSP70-1 IgG did not label the loops despite the signal being concentrated beneath the parasite surface, indicating that the parasite cytoplasm is not contained within the loops (Figure S4B).

WR induced trapping of exported reporter proteins increases PV loop formation

To resolve the extent to which WR treatment of the reporter lines induced the formation of PV loops, we treated Nluc-DH-Halo and Nluc-DH-APEX parasites -/+10 nM WR for 14-18 h and counted the loops. Although the super-resolution 3D cell reconstruction approach used previously was ideal for observing all the PV loops in a cell it was too time-consuming for large-scale analysis. Instead we imaged dozens of cells with widefield microscopy and deconvolution and counted the loops in just a single z plane at the widest point of the cell as delineated by EXP2 (Figure 4G). Although we found that in the absence of WR some Nluc-DH-Halo and Nluc-DH-APEX parasites contained loops, there were significantly more loops per cell when the cargo was trapped with WR (Nluc-DH-Halo: 0 nM WR, mean 0.10 SEM 0.06; 10 nM WR, mean 1.2 SEM 0.19. Nluc-DH-APEX: 0 nM WR, mean 0.14 SEM 0.06; 10 nM WR, mean 0.91 SEM 0.21) (Figure 4G).

We also examined late ring and early trophozoite stages corresponding to the period when the Nluc reporters began to be expressed. Expression of the Nluc-DH reporter first appeared in the ER before being exported into the erythrocyte (Figure S5). Small PV loops were observed in 17% of untreated parasites and in 35% of WR treated parasites. Loops were nearly always observed in young trophozoites containing small hemozoin deposits rather than in rings not containing hemozoin. In contrast, loops were observed in 9 and 10% of untreated Nluc-DH-APEX and Nluc-DH-Halo ~28 hpi trophozoites, respectively (Figure 4G). This increased to 63 and 73% respectively, following WR treatment.

Removal of the WR-induced trapping partially restored protein export.

Previous experiments with WR-trapped GFP-mDHFR reporter proteins indicated that once WR was removed there appeared to be no resumption of export of PV-trapped, fully folded GFP reporter into the erythrocyte [20]. Instead the work indicated that GFP reporters exported after WR removal were likely newly synthesised protein. Since the export assay with the Nluc reporter proteins provides a quantitative measure of trapping and export we re-examined resumption of protein export using these reporters. Ring stage parasites were treated with 0 or 10 nM WR and when trophozoites (~28 hpi) the drug was removed and the relative amount of reporter protein exported at 0, 2, 4 and 8 h afterwards was quantified by the export assay (Figure 5A). Removal of 10 nM WR led to a significant increase in export of the Nluc-DH fusion protein but only at 8 hours post drug removal (Figure 5A). Having additional protein domains on the Nluc-DH reporter was associated with opposite effects in the Nluc-DH-APEX and Nluc-DH-Halo parasites. The additional APEX

domain permitted a significant recovery of export only 2 h after WR removal in Nluc-DH-APEX parasites. In contrast in the Nluc-DH-Halo parasites there was no export recovery even after 8 h (Figure 5A). Interestingly, the recovered Nluc activity came from the parasite compartment rather than from the PV fraction (Figure 5A). This raised the question of whether the fraction of parasite reporter that was exported after WR removal was unfoldable protein trapped in the parasite or newly synthesised material that had not been affected by the WR.

One unexpected observation was that the parasite compartment fraction of the untreated Nluc-DH parasites at 25% of the total signal was much higher than the few per cent normally observed (Figure 5A). The parasite compartment signal for 10 nM WR treated was even higher at 50% of the total signal. We believe this may have been due to these parasites being several hours younger than estimated (~20 cf. 28 hpi, see also Figure S5) when the *eflα* promoter was just becoming active [21]. At this stage there may have been much more newly synthesised reporter in the parasite relative to the protein that had already been exported thereby increasing the relative contribution from the parasite compartment.

WR trapped Nluc-DH-APEX fusion protein exported 2 hours after drug removal is not newly synthesised protein.

The translation inhibitor cycloheximide (CHX) was used to prevent new protein synthesis to enable us to determine if the fraction of Nluc-DH-APEX exported into the parasite after WR removal was old or new material. To determine if the CHX was functioning as expected, Nluc-DH-APEX parasites were treated with and without 100 µM of the inhibitor and after 0.5 h, total Nluc activity was measured to establish baseline levels. After 2.5 h the total Nluc levels were measured again and without CHX were found to have increased by 25% (Figure 5B). In 100 µM CHX, Nluc levels only increased by 5% indicating the drug potently arrested translation (Figure 5B).

To determine the effects of CHX upon protein export, ring stage parasites were treated with 10 nM WR and when trophozoites, they were supplemented +/- CHX for 0.5 h. Export assays were then performed indicating the Nluc-DH-APEX report was trapped as expected (0 h, Figure 5C). The WR was then removed and an export assay was performed 2 h later. As anticipated, in parasites not treated with CHX there was an increase in the proportion of exported Nluc-DH-APEX and a relative decrease in parasite-trapped reporter (Figure 5C). In the CHX-treated parasites export of the Nluc-DH-APEX reporter increased to the same degree as in parasites not treated with CHX indicating that removal of WR allowed export of older previously blocked reporter and not newly synthesised reporter. The other reporter lines were not tested since the recovery of reporter export was insufficient within the 2 h period after WR removal. The origin of the increased reporter protein export observed for Nluc-DH parasites 8 h post WR removal was not tested using the CHX approach, as this length of translation inhibition would likely have been toxic.

The WR-trapped Nluc-DH-APEX and Nluc-DH-Halo reporters weakly reduce parasite growth.

We next investigated if WR-trapped forms of the Nluc-DH-APEX and Nluc-DH-Halo reporters could reduce parasite growth by clogging PTEX and presumably decreasing the efficient export of essential proteins. WR-trapping has previously been shown to be deleterious to parasite growth with some exported GFP-mDHFR reporters [19]. To explore this we treated ring stage Nluc-DH-APEX and Nluc-DH-Halo parasites with different concentrations of WR and harvested parasites at the trophozoite stage over multiple cycles. Parasite growth was measured by parasite lactate dehydrogenase activity [33] and compared to a no WR control at each time point (Figure 6A). At the lowest concentrations of 1.25 and 2.5 nM WR, growth of Nluc-DH-Halo parasites after five intraerythrocytic cell cycles was significantly decreased relative to the no WR control (Figure 6B). At the highest WR concentrations of 5 and 10 nM the growth of all lines was significantly reduced relative to the no WR controls although the effect was greater in the Nluc-DH-Halo and Nluc-DH-APEX parasites than in control parasites.

To determine whether trapping the construct in the PV prevents export of other proteins we performed fluorescence microscopy with the

Nluc-DH-Halo parasites. As the construct is under EF1α promoter the reporter protein is strongly expressed from 20 hpi onwards [21]. To investigate if there is inhibition of export of an endogenous protein we performed IFA with glycophorin binding protein 130 (GBP130) since it is similarly expressed as the reporter and later than most other PEXEL proteins whose expression peaks in rings [34]. Qualitatively WR treatment caused some GBP130 to colocalise with the Nluc-DH-Halo reporter at the PV but much of the GBP130 was still exported (Figure 6C). WR-induced trapping of the reporter therefore did not appear to robustly block the export of endogenous proteins and this is probably why parasite growth was not strongly reduced.

WR-trapped Nluc reporter proteins bind PTEX components.

To establish if more WR-trapped Nluc reporters than non-trapped reporters were bound to PTEX we performed co-immunoprecipitation assays of PTEX150-HA via its HA-epitope. Ring stage Nluc-DH infected erythrocytes were treated overnight +/- 10 nM WR and when trophozoites, were magnet purified from uninfected erythrocytes. Western blots confirmed the total levels of Nluc-DH were similar (Figure 7A). To increase the stringency of the PTEX150-HA immunoprecipitation it was performed in RIPR buffer containing the strong ionic detergents deoxycholate and SDS. To prevent PTEX and its cargo dissociating in this buffer, protein interactions in live parasites were covalently stabilised by treatment with the reduction sensitive crosslinker DSP (dithiobis(succinimidyl propionate). We have previously used this approach to determine that PTEX preferentially bound PEXEL tagged GFP rather than PV resident secreted GFP [2]. PTEX150-HA was then immunoprecipitated with anti-HA IgG beads and the co-precipitation of other PTEX components as well as Nluc-DH cargo was quantified by western blot analysis. This revealed that the PTEX was intact and contained EXP2 and HSP101 and that this was associated with greater levels of Nluc-DH following WR treatment than in untreated parasites (Figure 7B). In contrast, control immunoprecipitations with anti-GFP IgG beads captured very little PTEX or Nluc-DH (Figure 7B) but did capture GFP from similarly treated parasites expressing GFP (Figure 7C).

Immunoprecipitations were also performed on Nluc-DH-APEX and Nluc-DH-Halo trophozoites that had been treated +/-WR overnight. The trophozoites were first saponin lysed and all soluble PV and exported Nluc reporter proteins were washed out only leaving that bound to PTEX or trapped in the parasite. The cells were then lysed in less stringent Triton X-100 buffer and western blot analyses of the PTEX150-HA immunoprecipitations indicated both HSP101 and EXP2 were co-purified (Figure S6A). However only low levels of the Nluc-DH-Halo reporter were captured and no Nluc-DH-APEX could be detected at all.

To improve detection sensitivity the immunoprecipitation eluates were analysed by mass spectrometry based protein sequencing. For Nluc-DH-APEX parasites, more Nluc-DH-APEX peptides were detected in the PTEX150-HA pull-down for WR-treated parasites than for untreated parasites (Figure 7D, top left). This pattern was also observed in Nluc-DH-Halo parasites, where more peptides were detected in the PTEX150-HA pull-down following treatment with WR than in untreated parasites (Figure 7D, top right). These experiments were repeated and produced similar trends (Table S1). The Nluc reporter peptide counts for both experiments were combined and the pie charts beneath the column graphs clearly indicate much more of the reporters were engaged with PTEX when in their WR-induced unfoldable form than without WR (Figure 7D, bottom).

The mass spectrometry data clearly indicates that the Nluc reporters were likely bound to the full PTEX complex since HSP101, EXP2, PTEX88 and Trx2 peptides were detected (Figure 7D). It was therefore likely cargo becomes progressively trapped in the full PTEX complex as it becomes more difficult to unfold supporting PTEX's role as a protein translocon. PTEX associated proteins Pf113 and HSP70-x were also detected as well as some members of the PV-localised EPIC complex and their peptide counts were not very different +/- WR (Figure 7D)[15,18].

We also attempted reciprocal experiments where we utilised the Halotag in the Nluc-DH-Halo

protein. Parasite lysates were incubated with HaloLink resin to facilitate covalent binding of the Halotag fusion protein to the resin. The resin was treated with TEV protease to cleave the fusion protein upstream of the Halotag (Figure 1A) releasing a 51 kDa Nluc-DH fragment detected with Nluc IgG (Figure S6B). Although a little EXP2 was also co-precipitated with Nluc-DH-Halo, no PTEX150 and HSP101 were present. It is possible we could not detect binding of PTEX to Nluc-DH-Halo because the fusion protein when bound to PTEX during export may have been in an unfolded form in which the Halotag was non-functional and unable to bind to the Halolink resin.

PTEX150 and EXP2 bind similar levels of cargo despite both EXP2 and trapped cargo localising to the PVM loops.

Previous binding experiments with PTEX and GFP reporters indicated that EXP2 but not HSP101 bound WR-trapped reporter [19]. This finding is compatible with our observation that both EXP2 and trapped cargo proteins are localised to PVM loops that exclude other PTEX proteins. If within these loops the WR-trapped Nluc reporters were lodged inside putative EXP2 pores we would anticipate that isolation of EXP2 could co-purify substantially more cargo than PTEX150 and HSP101 that do not localise to the loops. To confirm this the *exp2* gene was appended with a HA tag sequence as per *ptex150* and was transfected with the Nluc-DH fusion protein. Western blots of purified erythrocytes infected with EXP2-HA/Nluc-DH parasites revealed they expressed the HA-tagged EXP2 target protein as well as the Nluc-DH fusion protein (Figure 7A). As observed for the other reporter parasites, WR supplementation had little effect on protein expression after half an intraerythrocytic cell cycle (Figure 7A).

Immunoprecipitation of PTEX150-HA and EXP2-HA and identification of co-purifying proteins by mass spectrometry indicated that there were more Nluc-DH peptides associated with the PTEX proteins when WR-tapped than when not (Figure 7E, top). Pie charts of the combined peptides counts from two experimental replicates clearly indicate as per the other Nluc fusion proteins, there were more Nluc-DH peptides co-precipitating when the reporters were WR-trapped (Figure 7E, bottom, Table S2).

If EXP2 was binding more WR-trapped Nluc-DH than PTEX150 the combined +WR peptide counts for PTEX150-HA and EXP2-HA immunoprecipitation replicates should have been greater for EXP2. Instead Nluc-DH peptide counts for PTEX150-HA versus EXP2-HA were very similar at 44 cf. 39, respectively (Figure 7C, bottom, Table S2). Both PTEX immunoprecipitations were of similar efficiencies with comparable numbers of HSP101 peptides coming down for the combined replicates (+WR peptides, EXP2-HA 347 cf. PTEX150-HA 475). It is therefore likely that WR-trapped cargo could be lodged within the whole PTEX complex in the PV and once segregated into the loops structures the cargo dissociates from EXP2 or that these loops only represent a minor proportion of the total population of EXP2 and cargo (Figure 8).

Discussion

Survival of *Plasmodium* spp. parasites inside host erythrocytes is dependent on host cell remodelling, facilitated by parasite protein trafficking through the PTEX complex [3]. While more is now known about the components of the PTEX complex itself, including their essentiality [11,12], not a great deal has been established about the mechanistic process of export itself. Here we have utilised a series of sensitive and quantifiable reporter proteins to better define export of cargo with different properties. We have demonstrated that trapped cargo colocalises with PTEX, particularly with EXP2, and appears to promote the appearance of PV loops containing trapped cargo protein that is segregated from both the host cytosol and parasitophorous vacuole space. Furthermore, through utilising quantifiable Nluc reporter constructs we have shown that ~ 50% of trappable reporter can be blocked from export at either the PV where it interacts with PTEX components, or within the parasite itself. We have shown here that the reversibility of this trapping appears to be dependent on the specific protein under investigation. Importantly addition of increasing concentrations of WR, which renders reporters progressively more difficult to unfold, presumably increases their association

with the PTEX, providing further evidence of the complex's role as a protein unfolding translocase.

It was previously shown that mDHFR-GFP reporters become partly trapped at the PV upon addition of WR, leading to the conclusion that protein unfolding is therefore necessary for export [19,20,27,28]. By incorporating Nluc into these constructs we have been able to quantify the profile of blockage, and then release, at a population level. Our data indicated that trapping not only occurred in the PV itself, but surprisingly also within the parasite, suggesting that the PV may become 'overloaded' with excess trapped protein causing a build-up of exported proteins throughout the secretory system of the parasite. It is also possible that some internally WR-trapped reporter could be lodged in the ER sec61 translocon particularly if PEXEL proteins are post-translationally transported into the ER compartment from the cytoplasm. The export assay also demonstrated that the degree of export of the reporter proteins can be regulated by adding different concentrations of WR as previously established for a mDHFR-GFP reporter [20].

Although attachment of additional APEX and Halo domains to the core Nluc-DH reporter proved of limited use for microscopy, these constructs did result in different export efficiencies. The efficiency of WR-induced blockage of export increased as follows: Nluc-DH-APEX > Nluc-DH > Nluc-DH-Halo. Interestingly, reporter export was most rapidly reinstated in the same order after WR removal. It is possible that without WR the Nluc-DH-APEX protein is more amenable to unfolding and export than the other reporters and therefore becomes more readily trapped at low levels of WR. The ease of unfolding may facilitate rapidly re-initiation of Nluc-DH-APEX export following WR removal.

Both widefield microscopy and SIM revealed that the trapped reporters were often confined to punctate domains within the PV, which overlapped with PTEX components. This was previously observed with mDHFR-GFP reporters in ring stage parasites and the phenomenon is conserved here in trophozoites expressing Nluc reporters [35]. A punctate distribution of PV-located reporter proteins [36] and PTEX components [35] have been reported previously, and referred to as a 'necklace of beads'. Examination of dozens of cell images acquired during the course of this study indicated that PTEX150 and HSP101 almost invariably had punctate distribution whilst EXP2 was only punctate in 24% of images. EXP2 was uniformly distributed about 60% of cells with the remainder having a mixed appearance. The Nluc reporters in WR-treated cells were punctate in 60% of cells with the rest being uniformly labelled. The punctate PTEX complexes could represent 'export zones' located at sites where exported proteins are deposited by the vesicular transport system into underlying regions of the parasite plasma membrane. As suggested previously, having PTEX concentrated at so-called 'export zones' could enhance the efficiency and selectivity of the translocation process [35]. The uniform labelling seen for EXP2 and trapped Nluc reporter could represent protein that is no longer restricted to the PTEX regions and is in the process of re-distribution to PVM loops.

PV loops often contained WR-trapped reporter protein and EXP2, but not the other PTEX components. Three-dimensional reconstructions using SIM reveals that the "loops" are spherical membranous structures. They are likely equivalent to structures observed by electron tomography, that are occasionally observed close to the PVM, even in parasites without the trapped reporters [37]. These loops did not appear contiguous with the parasite cytoplasm as they were not positive for the parasite cytosolic protein HSP70-1. They are probably examples of the tubulo-vesicular network (TVN) which are PVM derived projections that extend into the erythrocyte compartment and may even bud off from the main PVM enveloping the parasite [36,38,39]. EXP2 has previously been localised by immuno-electron microscopy to the PVM and to membranes in the erythrocyte cytoplasm [40] and here using SIM we confirm the TVN structures are positive for EXP2. Distinct membranous structures positive for EXP2 have also been observed in the cytoplasmic compartment of reticulocytes but not mature erythrocytes [41]. It would be interesting to determine if misfolded exported proteins could also be localised to these membranous structures however we did not have access to reticulocytes to confirm this.

Given that the TVN loops were not positive for PTEX150 and HSP101 and were more abundant in WR-treated parasites compared to age-matched untreated parasites, we hypothesise that the TVN could represent a mechanism to remove misfolded proteins from PTEX positive protein translocation sites in the PVM. It is interesting to note that TVN structures seem particularly well developed in parasites over-expressing difficult-to-unfold secreted GFP reporter proteins [36,38]. WR induced trapping of mDHFR-GFP reporter proteins has been previously observed to induce mobile and 'worm-like' protrusions of the PV in live cells [19]. Parasites might therefore sequester difficult-to-unfold proteins into the TVN to prevent inhibition of PTEX-associated export and growth reduction. Alternatively, the accumulation of trapped reporters and EXP2 into the TVN might be passive with the remainder of PTEX actively excluded from the TVN and retained within PV punctate regions for protein translocation.

In contrast to our PTEX observations in *P. falciparum,* the tagging of EXP2, HSP101 and PTEX88 with mCherry fluorescent protein or GFP in *P. berghei* indicated these proteins not only localised to the PV but also to membranous tubules extending from the PV [42]. These tubules were observed in live cells and are probably equivalent to the TVN loops we imaged in our fixed cells. It is possible that the differences observed are species specific and that PTEX components are not segregated in *P. berghe*i. Alternatively, the attachment of large fluorescent proteins (compared with the small HA epitope in *P. falciparum*) may have reduced the efficiency of PTEX assembly leading the fusion proteins to freely disperse throughout the PV-TVN network in *P. berghei*.

Our previous native protein gel analyses of PTEX, indicated that only about half of PTEX subunit proteins were assembled into the full sized >1200 kDa complex with the remainder existing as smaller homo-oligomers [15]. This suggested that PTEX could be a dynamic complex assembled from cargo-binding subunits which could engage the EXP2 pore at the PVM to initiate translocation of the cargo [15]. The ability to disassemble PTEX and recycle its subunits for other translocon complexes would be particularly useful when the complex becomes jammed with unfoldable cargo. A consequence of PTEX disassembly is that the trapped cargo may remain lodged in EXP2 pores triggering segregation into TVN structures. If the Nluc-DH reporter remained trapped in EXP2, we would have expected that immunoprecipitation of EXP2 from WR-treated parasites should have yielded larger amounts of trapped cargo than PTEX150 immunoprecipitations. Unexpectedly, the experiments indicated there was little difference between EXP2 and PTEX150 immunoprecipitations with similar levels of trapped Nluc-DH. This indicates that EXP2 and unfoldable Nluc-DH cargo are possibly not associated whilst in the TVN structures. This result stands in contrast to previous results indicating trapped mDHFR-GFP reporter proteins are bound to EXP2 but not HSP101 [19]. A key difference between these studies and ours is that we used mass spectrometry to detect binding rather than western blot which we have found to be less sensitive. Additionally, our Nluc-mDHFR reporters were soluble proteins and the GFP-mDHFR reporters used previously were fusions with transmembrane domain containing exported proteins (SBP1, MAHRP1 and REX2). When trapped with WR these transmembrane reporters would likely be retained in membranes where they could interact with EXP2. The addition of a HA-epitope to HSP101 may also reduce the efficiency with which was retained as part of the PTEX/GFP-mDHFR complex [19].

Interestingly, after removing WR and reinstating export, most of the trapped protein appeared to derive from the parasite compartment rather than the PV since the cytoplasmic Nluc pool declined more than the PV pool. Based on our observations that some of the trapped reporter proteins are localised with EXP2 to the TVN loops and away from the rest of PTEX, the spatial separation may ensure most of the segregated reporter is never exported. It could be that following the removal of WR, the only pre-existing reporter proteins that can be exported are poised at the ER or are in cytoplasmic vesicles possibly bound to chaperones, so they can be unfolded for export once delivered to the PV.

Although the WR-induced trapping of highly expressed reporter proteins appears to enhance the formation of PV loops, these TVN structures do form naturally particularly in older parasites

[37,39]. Although the TVN could naturally form to sequester an accumulating burden of aggregated endogenous proteins resistant to unfolding away from PTEX, the TVN could also have other functions. Foremost would be to increase the surface area of the PVM for enhanced exchange of low molecular weight molecules (eg, amino acids, purines, vitamins) as the parasite begins to grow and replicate. The fact that EXP2 can complement the loss of GRA17, a presumed nutrient pore in *Toxoplasma gondii* parasites supports an additional role for EXP2 in nutrient uptake [43]. We note however that once the TVN structures have detached from the PVM nutrient exchange would no longer be possible.

Interestingly, a study with fluorescent membrane dyes indicated PVM loops begin forming in rings before expanding to tubules in trophozoites [39]. We did not observe EXP2 or Nluc reporters accumulating in loops in ring stage parasites. Instead, we only observed this in trophozoites particularly as they aged and when export was blocked with WR. Whether WR induced blocking of reporter export induces *de novo* formation of PVM loops or favours the accumulation of proteins into membranous loops that have already formed awaits further investigation.

When the endogenous gene for the exported protein *sbp1* was appended with the sequence for mDHFR-GFP, this potently arrested parasite growth following treatment with 4 nM WR [19]. The probable reason was that the SBP-mDHFR-GFP fusion was clogging PTEX in all cells thereby preventing the export of other essential proteins. In contrast, we measured relatively weak growth inhibition following WR treatment for Nluc-DH-Halo and Nluc-DH-APEX reporters and a partial block of GBP130 export. This could be due to the fact that our Nluc reporters were expressed later in the intraerythrocytic cell cycle from ~20 hpi under the *ef1α* promoter from an episome compared with the endogenous *sbp1* promoter used previously that was expressed in all of the early ring cells [19,21]. As a consequence, many exported proteins would have already gained access to the erythrocyte compartment by the time the WR-trapped Nluc constructs were maximally expressed. Additionally, 10 nM WR only blocked the export of our reporters by 50% suggesting PTEX was not completely clogged and was able to continue exporting essential proteins.

Conclusion

Protein export is essential for parasite survival and data generated here suggests that the parasite could have multiple mechanisms to avoid growth arrest when exported proteins are trapped in the PTEX complex. Specifically, we have shown that artificially trapped cargo can be exported upon release of the trapping pressure (WR removal), presumably due to the action of unfoldases throughout the system allowing unfolding. Additionally, the appearance of TVN loops containing EXP2 and trapped reporter suggests that a segregation mechanism potentially exists for clearing blockages from the PTEX to ensure export of essential effector proteins can continue (Figure 8). These data suggest that the TVN loops seen upon trapping could represent 'molecular garbage bins' to help ensure parasite survival under times of stress when proteins are presented to the PTEX in an inappropriate state.

Materials and Methods

Parasite Culture

Plasmodium falciparum was cultured in human RBCs (Australian Red Cross Blood Bank, blood-group O^+) at 4% haematocrit in AlbuMaxII media (RPMI-HEPES, 0.5% AlbuMaxII [GIBCO], 0.2% $NaHCO_3$, 0.37 mM hypoxanthine) at 37°C as described previously [44].

Transgenic Parasite lines

pLuc-GFP-HA-DD24 [45] was digested with *Hind*III and *Bam*HI to excise the *hdhfr* sequence which was replaced with that of *blasticidin deaminase* (*bsd*). The Nluc-DH-APEX construct was made by inserting a synthetic DNA sequence encoding *hyp1-flag-nanoluciferase-mdhfr-ty1-apex* (Genscript) into the pLuc-GFP-HA-DD24-bsd plasmid after removing Luc-GFP-HA-DD24 via *Xho*I and *Mlu*I sites. The Nluc-DH-Halo plasmid was made by excising the *apex* sequence from

the Nluc-DH-APEX plasmid via *Avr*II and *Mlu*I and replacing with the *halotag* sequence amplified by PCR from pHTC HaloTag CMV-neo (Promega). The Nluc-DH plasmid was made by excising the *apex* sequence from Nluc-DH-APEX via *Avr*II and *Mlu*I ligating the DNA ends after blunting. The transgenic *P. falciparum* parasites expressing the various Nluc-DH plasmids were made by cultivating PTEX150-HA*glmS* parasites (strain CS2) [11], in erythrocytes electroporated with 100 µg of the plasmids as per [46]. Transgenic parasites were selected with 5 µg/mL blasticidin S.

Differential permeabilisation and western blot analysis of parasite proteins.

After 16 h treatment +/- 10 nM WR99210, trophozoites expressing Nluc reporters were separated from uninfected red blood cells via a MACS magnetic column (Milteni Biotech) in serum-free RPMI HEPES free. The +/- WR parasite were equally divided into 6 Eppendorf tubes and then pelleted (500 x g, 5'). Each pair of tubes was treated with recombinant equinatoxin (produced in-house diluted 1/100 from a HisTrap purified preparation at a dilution empirically determined to cause complete hemolysis); or equinatoxin and 0.03% saponin; or equinatoxin and 0.25% Triton X-100. All treatments were performed in PK buffer (50 mM Tris, 150 mM NaCl, 1 mM $CaCl_2$, pH 7.4) in a total volume of 500 µL. Parasites were incubated at RT for 10' with shaking at 800 rpm. Following incubation 100 µL of Proteinase K in PK buffer was added to one tube from each pair at a final concentration of 20 µg/mL. Mock treatments with 100 µL of the same buffer containing no protease, were performed for the other tubes. Proteinase K digestion proceeded for 15' at 37°C with shaking at 800 rpm. The Proteinase K was inhibited via the addition of 100 µL of Complete Protease Inhibitor Cocktail (Roche) made up at a high concentration of 2 tablets per 3 mL PK buffer with the addition of 1 mM PMSF. Soluble supernatant material was then separated from insoluble pellet material by centrifugation (1000 x g, 5'). The supernatants were concentrated seven-fold to 100 µL via 10 KDa MW cut off spin columns (MilliQ). Pellet and supernatant material was resuspended in reducing sample buffer and electrophoresed via NuPAGE Bis Tris SDS-PAGE 4-12% (Thermo Fisher) in MES buffer prior to electrotransfer for western blotting.

Nanoluciferase export assay

Approximately 12 hpi ring stage parasites were cultured for 16 h in the presence or absence of WR. Where indicated, WR treated parasites were washed twice in complete media without WR prior to replating (initial timepoints were measured immediately after washing). Cycloheximide treatment (100 µM) was initiated in the indicated experiments one hour prior to removing WR and washing cells, inhibition of protein synthesis was verified by measuring total NLuc signal in hyptonic lysis buffer (described below) at 0.5 and 2.5 hours post-treatment to measure the increase in signal. Parasites were adjusted to 1% parasitaemia and 1% haematocrit in complete media, 5 µL each culture were added to eight replicate wells of a 96 well plate. As a spike-in control to adjust for effects of different buffers, purified His-Nluc was added to 3D7 parasites not expressing Nluc to 333 pg/mL, this sample was also added to eight replicate wells. For each of the following four buffers, 90 uL was added to two wells of each sample: Tris-phosphate buffer (10 mM Tris-phosphate, 132 mM NaCl, 5 mM EDTA, 5 mM DTT, pH 7.4) was added to determine background lysis, Equinatoxin (EQT) buffer (10 mM Tris-phosphate pH 7.4, 132 mM NaCl, 5 mM EDTA, 5 mM DTT, 4.89 µg/mL purified EQT [empirically determined to release maximum signal from exported Nluc while releasing minimum signal from a secreted NLuc reporter]) was added to release Nluc exported into the RBC cytoplasm, Saponin buffer (10 mM Tris-phosphate, 132 mM NaCl, 5 mM EDTA, 5 mM DTT, 4.89 µg/mL purified EQT, 0.03% saponin, pH 7.4) was added to release Nluc localized to the PV and RBC cytoplasm. Hypotonic buffer (10 mM Tris-phosphate, 5 mM EDTA, 5 mM DTT, 0.2% Igepal CA-630, pH 7.4) was added to release total NLuc. In each well, 5 uL tris-phosphate buffer containing 1:50 Nanoglo substrate (Promega) was injected using a CLARIOStar multiwell reader (final dilution of Nanoglo 1:1000) prior to shaking the plate 30 s at 700 rpm, then reading luminescence at maximum gain (4095) for 1 s per well. All calculations were performed using the mean of both wells as technical replicates, propagating standard error from mean. Each well was normalized to the

spike-in control of the corresponding buffer. Background was then subtracted from EQT, Saponin and Hypotonic buffer for each sample. Localization was calculated as follows for each buffer after normalizing and subtracting background signal:

% Exported – EQT Buffer / Hypotonic Buffer * 100

% Secreted – (Saponin Buffer – EQT Buffer) / Hypotonic Buffer * 100

% Retained – (Hypotonic Buffer – Saponin Buffer) / Hypotonic Buffer * 100

Final values are of combined data from three biological replicates, of two technical replicates each. Statistical significance was determined by one-way analysis of variance (ANOVA), with Dunnett's correction comparing each sample to a control sample (without WR for WR titration, T=0 timepoint for recovery from washing experiments)

Immunofluorescence assays (IFA)

Parasites were pelleted and washed twice in PBS before a final 10 µL cell pellet was re-suspended in 1 mL PBS. The cells were added to the wells of a 24 well tissue culture plate containing a coverslip (13 mm) coated in 0.1% Poly-L-Lysine. After the cells had settled fixation was performed in 4% paraformaldehyde and 0.0075% glutaraldehyde as per [47]. Coverslips were washed with PBS and permeabilized in 0.1% Triton X100 in PBS for 15 min and then blocked with 3% bovine serum albumin (BSA) in PBS. Primary antibodies (Table S3) were diluted in 3% BSA/PBS and incubated for 2 h at RT. Samples were washed 3x with PBS and incubated with secondary antibodies (AlexaFluor), 1:2000 in 3% BSA/PBS for 1 h. Samples were washed as above and mounted in Vectashield with DAPI (4',6-diamidino-2-phenylindole). Images were taken with a Zeiss Axio Observer Z1 inverted widefield microscope and deconvolution performed with Zen software. Images were processed and analysed using open java source FIJI software. Sub-diffraction imaging was performed using Structured-Illumination Microscopy [32]. The super resolution images were collected using a Nikon N-SIM microscope equipped with 488, 561 and 640 nm lasers, an Andor iXON DU897 EM-CCD camera and a 100x oil immersion lens having a numerical aperture of 1.49. The z-series was acquired using NIS-Elements and analysed both using NIS-Elements and the open java source, ImageJ/FIJI.

Electron microscopy

Erythrocytes infected with Nluc-DH-APEX parasites were treated with either 0 or 10 nM WR99210. Parasites were harvested by magnetic separation at the trophozoite stage and were fixed in 2% paraformaldehyde, 0.0075% glutaraldehyde for 30 min. Samples were then washed in PBS and permeablised with equinatoxin II (0.33 mg/mL) in PBS, then fixed in 2% paraformaldehyde, 0.0075% glutaraldehyde. After quenching with 20 mM glycine in PBS, samples were washed twice in PBS and then treated with 0.5 mg/ml 3,3'-diaminobenzidine (DAB) in 50 mM Tris HCl, 0.03% H_2O_2 for 5 min. The samples were washed in PBS, fixed in 2% OsO_4, washed in H_2O then dehydrated in an ethanol series followed by 100% acetone. The parasite samples were then infiltrated with Procure epoxy resin for 24 h at 60°C before polymerisation with benzyldimethylamine for 48 h. Thin sections were stained with uranyl acetate and lead citrate and observed on a Tecnai Spirit electron microscope.

Halotag experiments

For imaging of the parasites, Nluc-DH-Halo parasites were incubated at 2% hematacrit in RPMI media (with no Albumax) containing Oregon Green Halotag ligand (1:1000, Promega) for 1 h. After washing in PBS the cells were settled onto to poly-L-lysine coated coverslips and were fixed and probed as indicated above. For pull down experiments lysates were made from whole magnet purified Nluc-DH-Halo trophozoites as described below in Immunoprecipitation Assays. After solubilisation in 0.25% TX100 the lysate was diluted down to 0.05% with PBS before addition to HaloLink beads (Promega) overnight. After washing in PBS, bound proteins were eluted from the beads by digestion with TEV protease following manufacturer's instructions (Life Technologies).

Western blotting

Infected erythrocytes at stages indicated were lysed in 0.09% saponin prior to washing in PBS containing Complete protease inhibitor cocktail tablets (Roche). Pellets were resuspended in non-reducing SDS-PAGE sample buffer. Prior to electrophoresis on pre-cast 4-12% acrylamide gradient bis-tris gels (Invitrogen) in 1xNuPAGE MOPS SDS running buffer. Proteins were transferred onto nitrocellulose and subsequently blocked with 1% casein in PBS prior to probing with specific antibodies (Table S3). Primary antibodies were detected with fluorescent goat anti-mouse and anti-rabbit IgGs or goat anti-chicken-HRP (Rockland Immunochemicals) and visualized with a LiCor Odyssey infrared imager.

Block and release export assay

Parasites were prepared as listed for the standard export assay. WR was added at late ring stage approximately 16 hpi and washed out at late trophozoite stage approximately 28 hpi. Parasites were put in buffers as listed above (buffer alone, with equinatoxin, with 0.03% saponin and equinatoxin, or with 0.2% NP40) and relative light units of all plates were measured immediately (time 0), two, four and eight hours later with CLARIOstar multimode plate reader. Experiments were repeated on at least three independent occasions and two technical replicates were completed per biological replicate.

Malstat growth assay

Lactate dehydrogenase activity (LDH) was measured to determine parasite biomass as described previously [33]. Briefly, parasites were synchronized and adjusted to 2% haematocrit and 1% parasitemia in 96 well plates with different concentrations of WR. Late trophozoite stage parasites were diluted 1/8, and the remainder was harvested and stored at -80°C. Samples were thawed for 4 h and 30 µL of sample added to 75µL Malstat mixture (0.083 M Tris pH 7.5, 185 mM lactic acid, pH7.5, 0.17% TX100, 0.83 mM acetylpyridine adenine dinucleotide (APAD), 0.17 mg/mL Nitroblue tetrazolium (NBT), 0.08 mg/mL phenozine ethosulfate (PES)). Samples were incubated in the dark at RT until a colour change occurred (~45 minutes). Absorbance was measured at 650 nm. The growth of treated parasites was compared to untreated parasites (100% growth) in each cycle.

Immunoprecipitation assays

HA immunoprecipitation assay: PTEX150-HA/Nluc-DH, EXP2-HA/Nluc-DH, Nluc-DH-APEX and Nluc-DH-Halo parasites were treated at ring stage +/- 10 nM WR for 16 h and were saponin lysed as outlined above. Cell pellets were resuspended in 25x pellet volume 0.25% TX100/PBS with Complete protease inhibitor cocktail tablets (lysis buffer) at room temperature for 1.5 h. Insoluble material was subsequently pelleted at 14,000g/10mins/4˚C. An aliquot of each lysate was removed (input sample) and remainder was added to anti-HA agarose (Sigma, washed three times in lysis buffer prior to use) prior to incubation overnight at 4˚C. Samples were subsequently pelleted and washed twice in lysis buffer, prior to transfer to micro-bio-spin columns and three additional washes in lysis buffer. Bound proteins were eluted in non-reducing sample buffer and input and eluted fractions were electrophoresed on 4-12% precast gradient gels. DSP crosslinking of parasites (1 mM) and subsequent immunoprecipitation in RIPR buffer (25mM Tris•HCl pH 7.6, 150 mM NaCl, 1% TX-100, 1% sodium deoxycholate, 0.1% SDS.) were performed as described in [2].

Mass Spectrometry

Following immunoprecipitation as described above, bead-bound proteins were denatured, reduced and alkylated prior to on-bead tryptic digestion. Digested peptides were bound to C18 resin (Pierce, ThermoFisher Scientific), washed, eluted and concentrated prior to analysis by LC-MS/MS using Orbitrap Lumos mass spectrometer (Thermo Scientific) fitted with nanoflow reversed-phase-HPLC (Ultimate 3000 RSLC, Dionex). The nano-LC system was equipped with an Acclaim Pepmap nano-trap column and an Acclaim Pepmap RSLC analytical column. 1 µL of the peptide mix was loaded onto the enrichment (trap) column at an isocratic flow of 5 µL/min of 3% CH_3CN containing 0.1% formic acid for 6 min before the enrichment column was switched in-line with the analytical column. The eluents used

for the LC were 0.1% v/v formic acid (solvent A) and 100% CH_3CN/0.1% formic acid v/v. The gradient used was 3% B to 20% B for 95 min, 20% B to 40% B in 10 min, 40% B to 80% B in 5 min and maintained at 80% B for the final 5 min before equilibration for 10 min at 3% B prior to the next sample. The mass spectrometer was equipped with a NanoEsi nano-electrospray ion source (Thermo Fisher, USA) for automated MS/MS. High mass accuracy MS data were obtained in a data-dependent acquisition mode with the Orbitrap resolution set at 75 000 and the top-ten multiply charged species selected for fragmentation by HCD (single-charged and double-charged species were ignored). The ion threshold was set to 15 000 counts for MS/MS. The CE voltage was set to 27. The resolution was set to 120000 at MS1 with lock mass of 445.12003 with HCD Fragmentation and MS2 scan in ion trap. Top 3 second method was used to select species for fragmentation. Singly charged species were ignored and an ion threshold triggering at 1e4 was employed. CE voltage was set to 1.9kv. The "protein scores" in Table S1,2 were generated by MASCOT.

Acknowledgments

We thank the Australian Red Cross Blood Bank for the provision of human blood, Jacobus Pharmaceuticals for providing WR99210 and Monash Micro Imaging and the Advanced Microscopy Facility, University of Melbourne. We also thank Freya Fowkes and Elisabeth Walsh-Wilkinson for analysis and technical assistance. We would like to acknowledge the generous assistance provided by Nicholas Williamson, Ching-Seng Ang, Sean O'Callaghan and Shuai Nie of the Mass Spectrometry and Proteomics Facility at The University of Melbourne, Bio21 Institute. The authors gratefully acknowledge funding from the Victorian Operational Infrastructure Support Program received by the Burnet Institute and for grants from the National Health and Medical Research Council of Australia (1068287, 1021560 and 637406).

Supplementary Information

Table S1. LC-MS/MS derived peptide counts of PTEX150-HA immunprecipitations from Nluc-DH-APEX and Nluc-DH-Halo trophozoites treated -/+ 10 nM WR.

Table S2. LC-MS/MS derived peptide counts of PTEX150-HA and EXP2-HA immunprecipitations from Nluc-DH expressing trophozoites treated -/+ 10 nM WR.

Table S3. Source and concentration of antibodies used in this study.

Figure S1: The growth of parasites expressing human DHFR was not substantially reduced by treatment with WR99210 (WR) over one intraerythrocytic cell cycle. (A) WR at the concentrations indicated was added to WR-resistant PTEX150-HA ring stage parasites (~12 hours post invasion, hpi) expressing Nluc-DH-APEX and Nluc (control) proteins. Giemsa stained images of the parasites when ~28 hpi indicated no obvious reduction in growth. (B) At the WR concentrations indicated lactate dehydrogenase (LDH) activity was measured for these parasite lines as a surrogate for parasite growth. The fold increase of LDH activity (OD650 nm) from trophozoite stage parasites over one intraerythrocytic cell cycle is shown.

Figure S2: Nluc-DH-APEX reporter protein line expresses Nluc and TY1 epitope. Western blots of *Plasmodium falciparum* Nluc-DH-APEX and control PTEX150-HA trophozoites were probed with rabbit anti-Nluc IgG and mouse Mab for TY1 showing these epitopes were only expressed in the reporter protein parasites and not in the control. Treatment with WR99210 does not affect levels of the reporter protein. A mouse monoclonal for EXP2 indicates equal protein loading in all the lanes. Protein markers in kDa are indicated on the right.

Figure S3: Transmission electron micrographs of Nluc-DH-APEX parasites showing membranous extensions induced by trapping protein cargo export. (A) Section through an Nluc-DH-APEX parasite treated with 10 nM WR99210 showing membranous extension indicated by arrows and enlarged in (B). Scale bars = 1 µm and 200 nm, respectively. (C) SIM immunofluorescence image of parasite labelled for Nluc and EXP2 showing that the large loops (arrows) seen in A, B are not exceptional. (D, E) Membranous extensions were not observed in Nluc-DH-APEX parasites not treated with WR99210. Scale bar = 1 µm. The infected erythrocytes were treated with the pore forming protein equinatoxin, to release and remove haemoglobin prior to fixation to prevent haemoglobin activating the peroxidase substrate. Scale bar = 1 µm.

Figure S4. HSP101 and HSP70-1 do not localise to the EXP2 PV loops formed in WR-treated Nluc-DH trophozoites. (A) Nluc-DH rings were treated with 10 nM WR and when trophozoites were fixed and probed with an EXP2 mouse monolconal and rabbit anti-HSP101 IgG. Widefield immunfluoroescence imaging reveals HSP101 localises to the PV (arrows) but not to the EXP2 PV loops. (B) Parasites similarly treated were also probed for the parasite cytoplasmic HSP70-1 protein that did not localise to the EXP2 labelled PV loops indicating they did not contain parasite cytoplasm.

Figure S5. Nluc-DH begins to be expressed in late ring to early trophozoite stage parasites in the peri-nuclear endoplasmic reticulum.

Some export of the reporter protein into the erythocye compartment was observed in 33% of cells (n=46); generally young trophozoites as determined by the presence of small hemozoin bodies. Overnight treatment with 10 nM WR reduced export that was only obseved in 3% of parasites (n=33). One or two loops were observed in 35% of WR-treated and 17% of untreated parasites, nearly all of which were trophozoites. Scale bar = 5 μm

Figure S6. NLuc-DH-Halo reporter protein binds to the PTEX complex. (A) Co-immunprecipitation experiments were performed by pulling down PTEX150-HA with anti-HA IgG in the PTEX150-HA control parasites as well as the Nluc-DH-APEX and Nluc-DH-Halo parasites which also contain HA-tagged PTEX150. In the -/+ WR-treated Nluc-DH-Halo parasites PTEX150, EXP2 and HSP101 were precipitated (Elute) as well as the Nluc reporter protein. Nluc-DH-APEX was probably below the limits of detection in the Elute fractions and so a more sensitive mass spectrometry based approach was used. (B) Lysate from WR-trapped Nluc-DH-Halo parasites was covalently bound to HaloLink resin and then eluted with TEV protease followed by non-reducing protein sample buffer (NRSB). Although the Nluc-DH fragment of the full-length fusion protein was eluted only EXP2 and not PTEX150 or HSP101 could be identified as bound to the reporter protein.

Videos S1 and S2. Three-dimensional rotations of serial sections through Nluc-DH trophozoites treated with 10 nM WR99210 and stained for Nluc (green) and EXP2 (red). The optical sections were performed using structured illumination microscopy (SIM) and correspond to the images shown in Figure 4A, B.

Videos S3 and S4. Three-dimensional rotations of serial sections through Nluc-DH trophozoites treated with 10 nM WR99210 and stained for Nluc (green) and PTEX150 (red). The optical sections were performed using structured illumination microscopy (SIM) and correspond to the images shown in Figure 4C, D.

References

1. World Malaria Report. 2016.
2. de Koning-Ward TF, Gilson PR, Boddey JA, et al. A newly discovered protein export machine in malaria parasites. *Nature.* 2009;459(7249):945-949.
3. de Koning-Ward TF, Dixon MW, Tilley L, Gilson PR. Plasmodium species: master renovators of their host cells. *Nat Rev Microbiol.* 2016;14(8):494-507.
4. Boddey JA, Cowman AF. *Plasmodium* Nesting: Remaking the Erythrocyte from the Inside Out. *Annual Review of Microbiology.* 2013;67(1):243-269.
5. Boddey JA, Hodder AN, Gunther S, et al. An aspartyl protease directs malaria effector proteins to the host cell. *Nature.* 2010;463(7281):627-631.
6. Boddey JA, Moritz RL, Simpson RJ, Cowman AF. Role of the *Plasmodium* Export Element in Trafficking Parasite Proteins to the Infected Erythrocyte. *Traffic.* 2009;10(3):285-299.
7. Marti M, Good RT, Rug M, Knuepfer E, Cowman AF. Targeting Malaria Virulence and Remodeling Proteins to the Host Erythrocyte. *Science.* 2004;306(5703):1930-1933.
8. Hiller NL, Bhattacharjee S, van Ooij C, et al. A host-targeting signal in virulence proteins reveals a secretome in malarial infection. *Science.* 2004;306(5703):1934-1937.
9. Chang HH, Falick AM, Carlton PM, Sedat JW, DeRisi JL, Marletta MA. N-terminal processing of proteins exported by malaria parasites. *Molecular and Biochemical Parasitology.* 2008;160(2):107-115.
10. Boddey JA, Carvalho TG, Hodder AN, et al. Role of Plasmepsin V in Export of Diverse Protein Families from the *Plasmodium falciparum* Exportome. *Traffic.* 2013;14(5):532-550.
11. Elsworth B, Matthews K, Nie CQ, et al. PTEX is an essential nexus for protein export in malaria parasites. *Nature.* 2014;511(7511):587-591.
12. Beck JR, Muralidharan V, Oksman A, Goldberg DE. PTEX component HSP101 mediates export of diverse malaria effectors into host erythrocytes. *Nature.* 2014;511(7511):592-595.

13. Bullen HE, Charnaud SC, Kalanon M, et al. Biosynthesis, Localization, and Macromolecular Arrangement of the *Plasmodium falciparum* Translocon of Exported Proteins (PTEX). *J Biol Chem.* 2012;287(11):7871-7884.
14. Hakamada K, Watanabe H, Kawano R, Noguchi K, Yohda M. Expression and characterization of the Plasmodium translocon of the exported proteins component EXP2. *Biochem Biophys Res Commun.* 2017;482(4):700-705.
15. Elsworth B, Sanders PR, Nebl T, et al. Proteomic analysis reveals novel proteins associated with the *Plasmodium* protein exporter PTEX and a loss of complex stability upon truncation of the core PTEX component, PTEX150. *Cellular Microbiology.* 2016;18:1551-1569.
16. Matz JM, Ingmundson A, Costa Nunes J, Stenzel W, Matuschewski K, Kooij TWA. In Vivo Function of PTEX88 in Malaria Parasite Sequestration and Virulence. *Eukaryotic Cell.* 2015;14(6):528-534.
17. Chisholm SA, McHugh E, Lundie R, et al. Contrasting Inducible Knockdown of the Auxiliary PTEX Component PTEX88 in P. falciparum and P. berghei Unmasks a Role in Parasite Virulence. *PLoS One.* 2016;11(2):e0149296.
18. Batinovic S, McHugh E, Chisholm SA, et al. An exported protein-interacting complex involved in the trafficking of virulence determinants in Plasmodium-infected erythrocytes. *Nat Commun.* 2017;8:16044.
19. Mesen-Ramirez P, Reinsch F, Blancke Soares A, et al. Stable Translocation Intermediates Jam Global Protein Export in Plasmodium falciparum Parasites and Link the PTEX Component EXP2 with Translocation Activity. *PLoS Pathog.* 2016;12(5):e1005618.
20. Gehde N, Hinrichs C, Montilla I, Charpian S, Lingelbach K, Przyborski JM. Protein unfolding is an essential requirement for transport across the parasitophorous vacuolar membrane of *Plasmodium falciparum*. *Molecular Microbiology*. 2009;71(3):613-628.
21. Azevedo MF, Nie CQ, Elsworth B, et al. Plasmodium falciparum transfected with ultra bright NanoLuc luciferase offers high sensitivity detection for the screening of growth and cellular trafficking inhibitors. *PLoS One.* 2014;9(11):e112571.
22. Counihan N, Chisholm S, Bullen H, et al. Plasmodium parasites deploy RhopH2 into the host erythrocyte to obtain nutrients, grow and replicate. *eLife.* 2017;e23217.
23. Dickerman BK, Elsworth B, Cobbold SA, et al. Identification of inhibitors that dually target the new permeability pathway and dihydroorotate dehydrogenase in the blood stage of Plasmodium falciparum. *Sci Rep.* 2016;6:37502.
24. Buskes MJ, Harvey KL, Richards BJ, et al. Antimalarial activity of novel 4-cyano-3-methylisoquinoline inhibitors against Plasmodium falciparum: design, synthesis and biological evaluation. *Org Biomol Chem.* 2016;14(20):4617-4639.
25. Weiss GE, Gilson PR, Taechalertpaisarn T, et al. Revealing the sequence and resulting cellular morphology of receptor-ligand interactions during Plasmodium falciparum invasion of erythrocytes. *PLoS Pathog.* 2015;11(2):e1004670.
26. De Niz M, Stanway RR, Wacker R, Keller D, Heussler VT. An ultrasensitive NanoLuc-based luminescence system for monitoring Plasmodium berghei throughout its life cycle. *Malar J.* 2016;15:232.
27. Grüring C, Heiber A, Kruse F, et al. Uncovering Common Principles in Protein Export of Malaria Parasites. *Cell Host & Microbe.* 2012;12(5):717-729.
28. Heiber A, Kruse F, Pick C, et al. Identification of New PNEPs Indicates a Substantial Non-PEXEL Exportome and Underpins Common Features in *Plasmodium falciparum* Protein Export. *PLoS Pathogens.* 2013;9(8):e1003546.
29. Hung V, Zou P, Rhee HW, et al. Proteomic mapping of the human mitochondrial intermembrane space in live cells via ratiometric APEX tagging. *Mol Cell.* 2014;55(2):332-341.
30. Los GV, Wood K. The HaloTag: a novel technology for cell imaging and protein

analysis. *Methods Mol Biol.* 2007;356:195-208.
31. Jackson KE, Spielmann T, Hanssen E, et al. Selective permeabilization of the host cell membrane of Plasmodium falciparum-infected red blood cells with streptolysin O and equinatoxin II. *Biochem J.* 2007;403(1):167-175.
32. Gustafsson MG. Nonlinear structured-illumination microscopy: wide-field fluorescence imaging with theoretically unlimited resolution. *Proc Natl Acad Sci U S A.* 2005;102(37):13081-13086.
33. Makler MT, Hinrichs DJ. Measurement of the lactate dehydrogenase activity of Plasmodium falciparum as an assessment of parasitemia. *Am J Trop Med Hyg.* 1993;48(2):205-210.
34. Bozdech Z, Llinás M, Pulliam BL, Wong ED, Zhu J, DeRisi JL. The Transcriptome of the Intraerythrocytic Developmental Cycle of *Plasmodium falciparum*. *PLoS Biol.* 2003;1(1):e5.
35. Riglar DT, Rogers KL, Hanssen E, et al. Spatial association with PTEX complexes defines regions for effector export into *Plasmodium falciparum*-infected erythrocytes. *Nature Comm.* 2013;4:1415.
36. Adisa A, Rug M, Klonis N, Foley M, Cowman AF, Tilley L. The signal sequence of exported protein-1 directs the green fluorescent protein to the parasitophorous vacuole of transfected malaria parasites. *J Biol Chem.* 2003;278(8):6532-6542.
37. Hanssen E, Carlton P, Deed S, et al. Whole cell imaging reveals novel modular features of the exomembrane system of the malaria parasite, *Plasmodium falciparum*. *International Journal for Parasitology.* 2010;40(1):123-134.
38. Wickham ME, Rug M, Ralph SA, et al. Trafficking and assembly of the cytoadherence complex in *Plasmodium falciparum*-infected human erythrocytes. *EMBO Journal.* 2001;20(20):5636-5649.
39. Elmendorf HG, Haldar K. Plasmodium falciparum exports the Golgi marker sphingomyelin synthase into a tubovesicular network in the cytoplasm of mature erythrocytes. *J Cell Biol.* 1994;124(4):449-462.
40. Johnson D, Günther K, Ansorge I, et al. Characterization of membrane proteins exported from *Plasmodium falciparum* into the host erythrocyte. *Parasitology.* 1994;109(01):1-9.
41. Meibalan E, Comunale MA, Lopez AM, et al. Host erythrocyte environment influences the localization of exported protein 2, an essential component of the Plasmodium translocon. *Eukaryot Cell.* 2015;14(4):371-384.
42. Matz JM, Goosmann C, Brinkmann V, et al. The *Plasmodium berghei* translocon of exported proteins reveals spatiotemporal dynamics of tubular extensions. *Scientific Reports.* 2015;5:12532.
43. Gold DA, Kaplan AD, Lis A, et al. The *Toxoplasma* Dense Granule Proteins GRA17 and GRA23 Mediate the Movement of Small Molecules between the Host and the Parasitophorous Vacuole. *Cell Host & Microbe.* 2015;17(5):642-652.
44. Trager W, Jensen JB. Human malaria parasites in continuous culture. *Science.* 1976;193(4254):673-675.
45. de Azevedo MF, Gilson PR, Gabriel HB, et al. Systematic analysis of FKBP inducible degradation domain tagging strategies for the human malaria parasite Plasmodium falciparum. *PLoS One.* 2012;7(7):e40981.
46. Hasenkamp S, Russell KT, Horrocks P. Comparison of the absolute and relative efficiencies of electroporation-based transfection protocols for Plasmodium falciparum. *Malar J.* 2012;11:210.
47. Tonkin CJ, van Dooren GG, Spurck TP, et al. Localization of organellar proteins in Plasmodium falciparum using a novel set of transfection vectors and a new immunofluorescence fixation method. *Mol Biochem Parasitol.* 2004;137(1):13-21.

Figures

Figure 1. Diagrams of export reporter gene constructs used to transfect *Plasmodium falciparum.* (A) Gene cassettes joined together to encode the Nluc-DH (top), Nluc-DH-APEX (middle) and Nluc-DH-Halo (bottom) fusion proteins. All constructs were inserted into the blasticidin deaminase (BSD) drug selection plasmid pEF, under the control of the *ef1α* promoter. PEXEL and TEV protease cleavage sites are indicated. The expected sizes of the various parts of the constructs are indicated in kDa (top) and amino acids (bottom). (B) Western blot analysis of *P. falciparum* trophozoites transfected with gene constructs following overnight treatment +/- 10 nM WR99210. Left, kDa of protein markers and Right, antibody probes.

Figure 2. Export of Nluc reporters are blocked in the PV with WR in a concentration dependent manner. (A) Western blot analysis of differentially permeabilised Nluc-DH-Halo trophozoites previously treated +/- WR for 16 h. After permeabilisation with equinatoxin II (EqtII), saponin (Sap) or Triton X-100 (TX100) to expose red blood cell (RBC), RBC and PV or all cellular proteins respectively, the cells were treated +/- 20 µg/mL proteinase K. The cell lysates were then centrifuged to separate soluble (S) and pellet (P) fractions that were separated by SDS-PAGE. Western blots were probed with various IgGs (right) and molecular markers are on the left. (B) Diagram highlighting similarities and differences of the protein export assays used in (A, Top) versus (C, Bottom). The membranes of the infected erythrocyte were similarly permeabilised in both assays. In (A), the susceptibility of the Nluc cargo proteins to Proteinase K proteolysis was assessed by western blot and in (C) the ability of the Nluc proteins to access their NanoGlo substrate was being measured. (C) Nluc-DH, Nluc-DH-APEX and Nluc-DH-Halo and Nluc control parasites, expressing exported nanoluciferase (Nluc), were treated with different concentrations of WR99210 (WR) for 16 h at ring stage. At the late trophozoite stage (~28 hpi) bioluminescence activity of the Nluc reporter was measured after differentially lysing the erythrocyte (exported), PV and parasite cytoplasmic compartments. Export of the reporter proteins was blocked with WR in a concentration dependent manner, and there was a significant decrease observed in export with some WR concentrations compared with untreated parasites. *p<0.05, **p<0.01, ***p<0.001, ****p<0.0001. The exported Nluc reporter expressed in the control line, lacks a mDHFR and shows no significant WR-induced inhibition of export. P values were calculated by one-way analysis of variance (ANOVA) with Dunnett's correction. Three independent biological replicates were performed, each with two technical replicates. Error bars represent standard error of the mean.

Figure 3. Widefield immunofluorescence microscopy of Nluc-DH, Nluc-DH-APEX and Nluc-DH-Halo trophozoites reveals treatment with WR99210 blocks protein export into the erythrocyte compartment. (A-C) Parasite lines imaged are indicated on the left, antibody probes are shown at the top of the image panels and the concentration of WR used is on the right. For Nluc-DH-Halo the Halotag was stained with the Oregon green dye. White arrows indicate the EXP2 and trapped reporter protein loops appearing to project from the parasitophorous vacuole membrane. (D) A selection of Nluc-DH parasites treated -/+ WR showing Nluc (green) trapped within the parasite especially around the nuclei (blue). Scale bar = 5 µm. DIC, Differential interference contrast; BF, Brightfield.

Figure 4. Structured illumination microscopy of WR-treated Nluc-DH trophozoites showing trapped cargo proteins localising with PTEX proteins in the PVM. (A, B) (Top) Single z optical sections of parasites stained with anti-Nluc and anti-EXP2 IgGs showing both proteins colocalised to PV puncta and loops projecting from the PVM that are indicated with white arrows. (Bottom) Maximum intensity projections of serial optical z sections showing both proteins colocalised into punctate regions on the parasite surface. (C, D) (Top) Single sections of Nluc-DH parasites stained with anti-Nluc and anti-PTEX150-HA IgGs showing both proteins localise to PV puncta but PTEX150 does not colocalise to

the surface loops. (Bottom) maximum intensity projections showing both proteins localise to surface micro-domains. Yellow arrow in maximum projection of (D) indicates second parasite co-infecting the erythrocyte. Scale bars = 1 µm. (E, F) Respective SIM and widefield images of HSP101-HA trophozoites not transfected with Nluc reporters probed for EXP2 and HSP101 via HA monoclonal IgG. Arrows indicate small EXP2 positive PVM loop 'buds' that do not stain for HSP101. Blue arrows in (F) indicate perinuclear HSP101 labelling. Scale bars for SIM (E) and widefield (F) images are 1 and 5 µM, respectively. (G) Number of Nluc positive loops seen in 0 and 10 nM WR samples in both Nluc-DH-Halo (left) and Nluc-DH-APEX (right). n = number of cells analysed, Mann-Whitney analysis where **p=0.0001, *** p<0.0001.

Figure 5. Export recovery of pre-synthesised Nluc reporter proteins after removal of WR99210 is reporter construct dependent. (A) Ring stage parasites were treated -/+ 10 nM WR and when late trophozoites (~28 hpi) the WR was removed. After 0, 2, 4 and 8 h Nluc activity was measured by the export assay. *p<0.05, **p<0.01, ***p<0.001, ****p<0.0001. p values were calculated by one-way analysis of variance (ANOVA) with Dunnett's correction. Experiments were repeated on three independent occasions and two technical replicates were completed per biological replicate. Error bars represent standard error of the mean. (B) To determine if the Nluc reporter proteins exported after WR removal, were old or newly made proteins, export assays were performed following treatment with the translation inhibitor Cycloheximide (CHX). To confirm that CHX functioned as intended +/- 100 µM of the drug was added to inhibit protein synthesis at the late trophozoite stage (~28 hpi). Half an hour later (0.5 h) total Nluc activity was measured to establish a baseline. Two hours later (2.5 h) the increase in total bioluminescence signal was measured to determine how much CHX inhibited of protein synthesis. The experiment was repeated three times and error bars represent error weighted SD. (C) (Left) To determine if export recovery in WR-treated (10 nM) Nluc-DH-APEX parasites after WR removal was due to pre-existing or newly synthesised protein the export assay was performed on parasites treated +/- 100 µM CHX. Half an hour after CHX addition baseline export was established and the WR was removed (0 h). After 2 h, export was measured again there was a significant degree of export recovery (***p<0.001) in parasites treated with and without CHX. Importantly, there was no significant difference (NS) observed between export -/+ CHX suggesting most of the protein exported was pre-existing. P value was calculated using an unpaired Student's t test. Experiments were repeated three times with two technical replicates per assay. Error bars represent error weighted SD.

Figure 6. WR induced trapping of Nluc-DH-Halo and Nluc-DH-APEX reporters leads to reduced parasite growth over five intraerythrocytic cell cycles. (A) Nluc-DH-Halo, Nluc-DH-APEX and Nluc control parasites were synchronized at ring stage and treated with different concentrations of WR as indicated. Trophozoite stage parasites were harvested at each of five intraerythrocytic cell cycles of WR treatment and then lactate dehydrogenase activity was measured. Growth was calculated as a percentage compared to growth in no WR (0 nM) at each time point. Data is representative of three independent experiments done in triplicate and error bars represent SD. (B) Mean percentage growth after 4 cycles at various WR concentrations compared to no WR. 2 way ANOVA of growth compared to 0 nM WR with **p<0.01, ***p<0.001, ****p<0.0001. (C) Widefield immunofluorescence images of 0 and 10 nM WR-treated Nluc-DH-Halo trophozoites stained with rabbit anti-Nluc IgG and a mouse monoclonal for GBP130. Although Nluc-DH-Halo is trapped there is no substantial trapping of GBP130. Scale bar = 5 µm

Figure 7. Co-immunoprecipitation experiments indicate more Nluc reporter proteins are bound to PTEX when trapped with WR99210. (A) Western blots of whole erythrocytes infected with PTEX150-HA and EXP2-HA trophozoites expressing the Nluc-DH reporter. Anti-HA chicken IgY indicates PTEX150-HA and EXP2-HA parasites have been

successfully tagged and express the Nluc-DH reporter protein. Anti-EXP2 IgG indicates all lanes are similarly loaded and there is no difference -/+ 10 nM WR treatment for 16 h. (B) Immunoprecipitation of PTEX150-HA from whole magnet purified Nluc-DH parasites treated +/- 10 nM WR indicates more of the reporter associates with PTEX when trapped with WR. Two western blot panels probed with anti-Nluc IgG are shown. Control immunoprecipitations with anti-GFP IgG beads did not purify substantial amounts of PTEX or reporter. Asterisks indicate non-specific bands recognised by the anti-HA IgY and HSP101 IgG. (C). Immunoprecipitation with anti-GFP IgG beads on +/-WR treated Nluc-DH parasites and secreted GFP (SS-GFP) parasites indicates only GFP is purified. (D) PTEX150-HA was immunoprecipitated from parasites expressing the Nluc-DH-APEX and Nluc-DH-Halo reporters following treatment +/- 10nM WR99210. The immunoprecipitation eluates were subjected to LC-MS/MS based protein sequencing which identified all five PTEX components as well as as bound Nluc-DH-APEX and Nluc-DH-Halo reporters particularly when trapped with WR. The graphs show the number of peptides matching their respective proteins (log2 scale) and are representative of one of two experiments. Red text indicates the primary immunoprecipitation target. (A, Bottom) Pie graphs showing the proportions of Nluc reporter peptides from parasites treated +/-WR co-precipitating with PTEX150-HA. The peptide numbers from two combined biological replicates are shown. (E, Top) Protein peptide counts of anti-HA immunoprecipitations from PTEX150-HA/Nluc-DH and EXP2-HA/Nluc-DH trophozoites treated -/+ 10 nM WR99210. Binding of the Nluc-DH reporter to the PTEX proteins was greater when WR-trapped than when not. The number of reporter peptides binding to either PTEX protein was similar. Representative graph of one of two experiments is shown and red text indicates the primary immunoprecipitation target. (E, Bottom) Pie graphs showing the proportions of Nluc-DH reporter peptides from parasites treated +/-WR co-precipitating with PTEX150-HA and .EXP2-HA The peptide numbers from two combined biological replicates are shown.

Figure 8. Diagram showing how parasites putatively export proteins into their erythrocyte host via PTEX and cope with blocked PTEX complexes. (Left) Exported proteins are delivered to PTEX enriched export zones (red) at the parasite surface via vesicular transport. HSP101 and PTEX150 presumably assemble on the proteins and deliver them to EXP2 through which they are exported in an unfolded form. (Right) When mDHFR containing exported proteins are made refractory to unfolding by addition of WR99210, the reporter proteins accumulate in the PV at the export zones. The blocked proteins gradually migrate to PVM extensions called the tubulo-vesicular network (TVN) along with EXP2 but not the rest of PTEX. The blocked reporter proteins once spatially segregated from the export zones cannot be exported when the WR ligand is removed. The disassembly of PTEX allows all the non-EXP2 components to be recycled for further export.

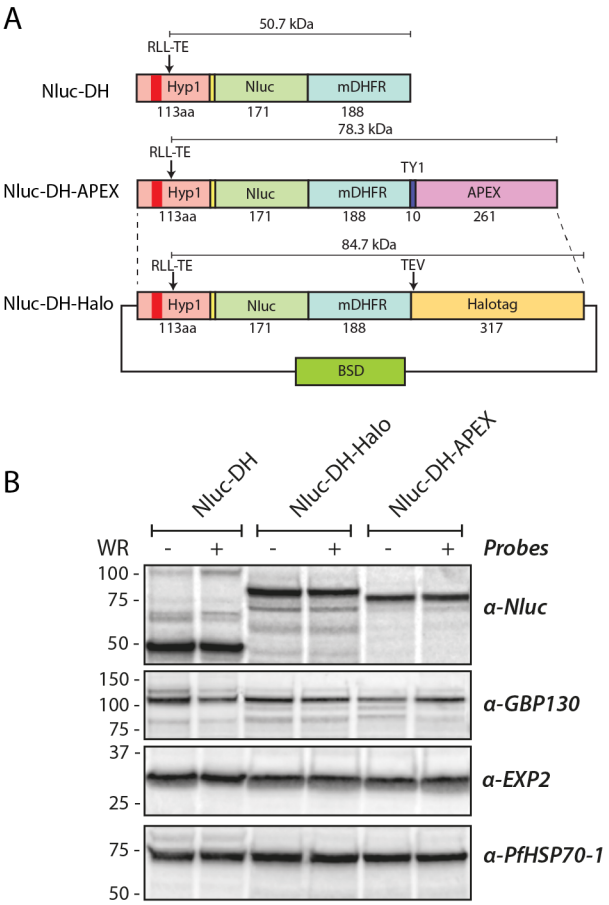

Fig 1.tif

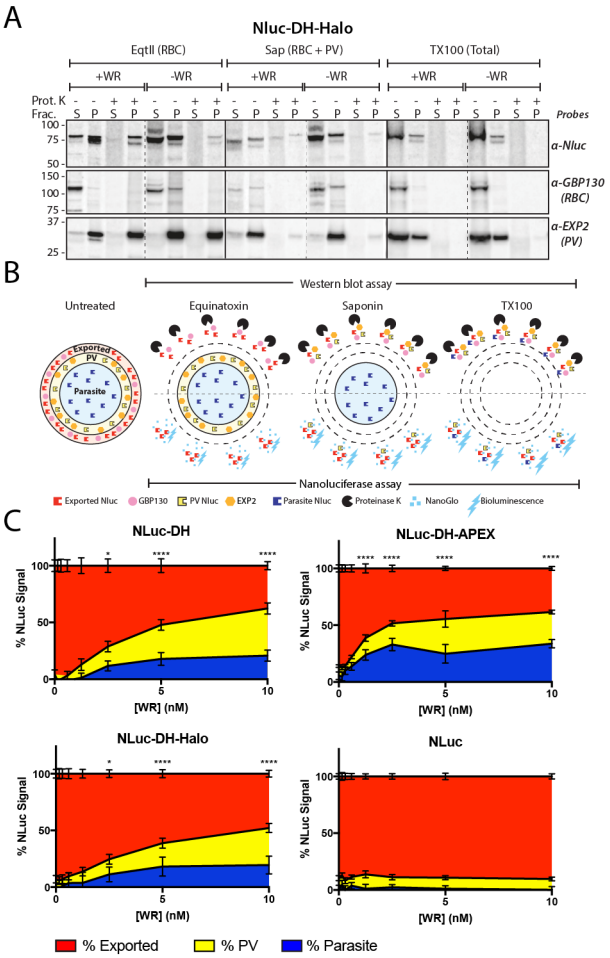

Fig 2.tif

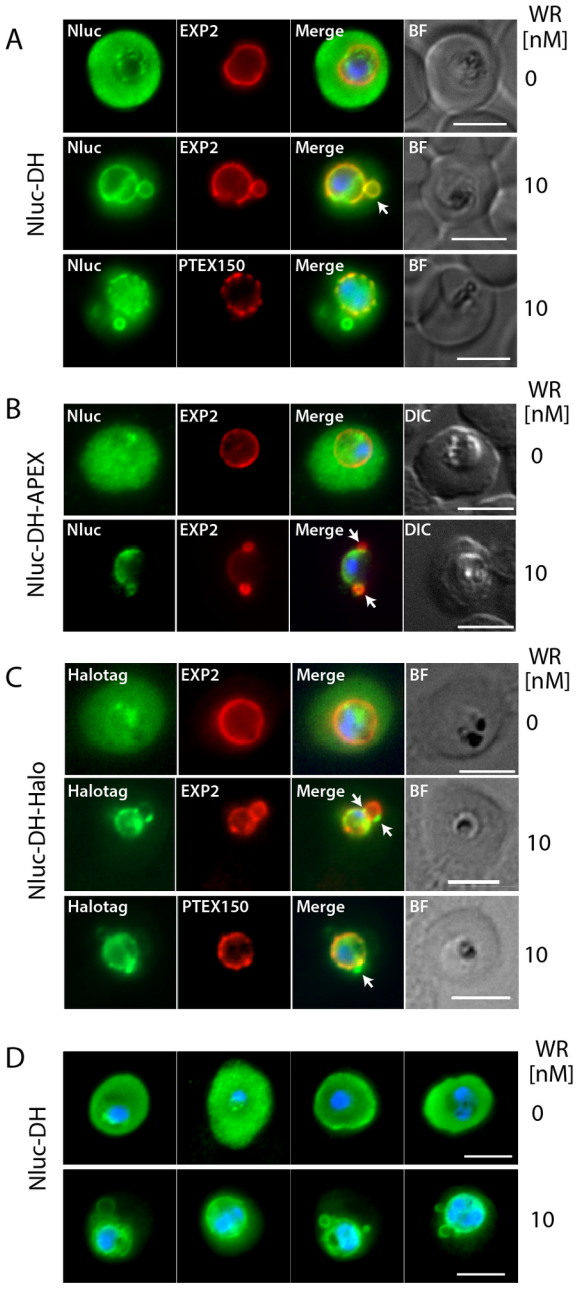

Fig 3.tif

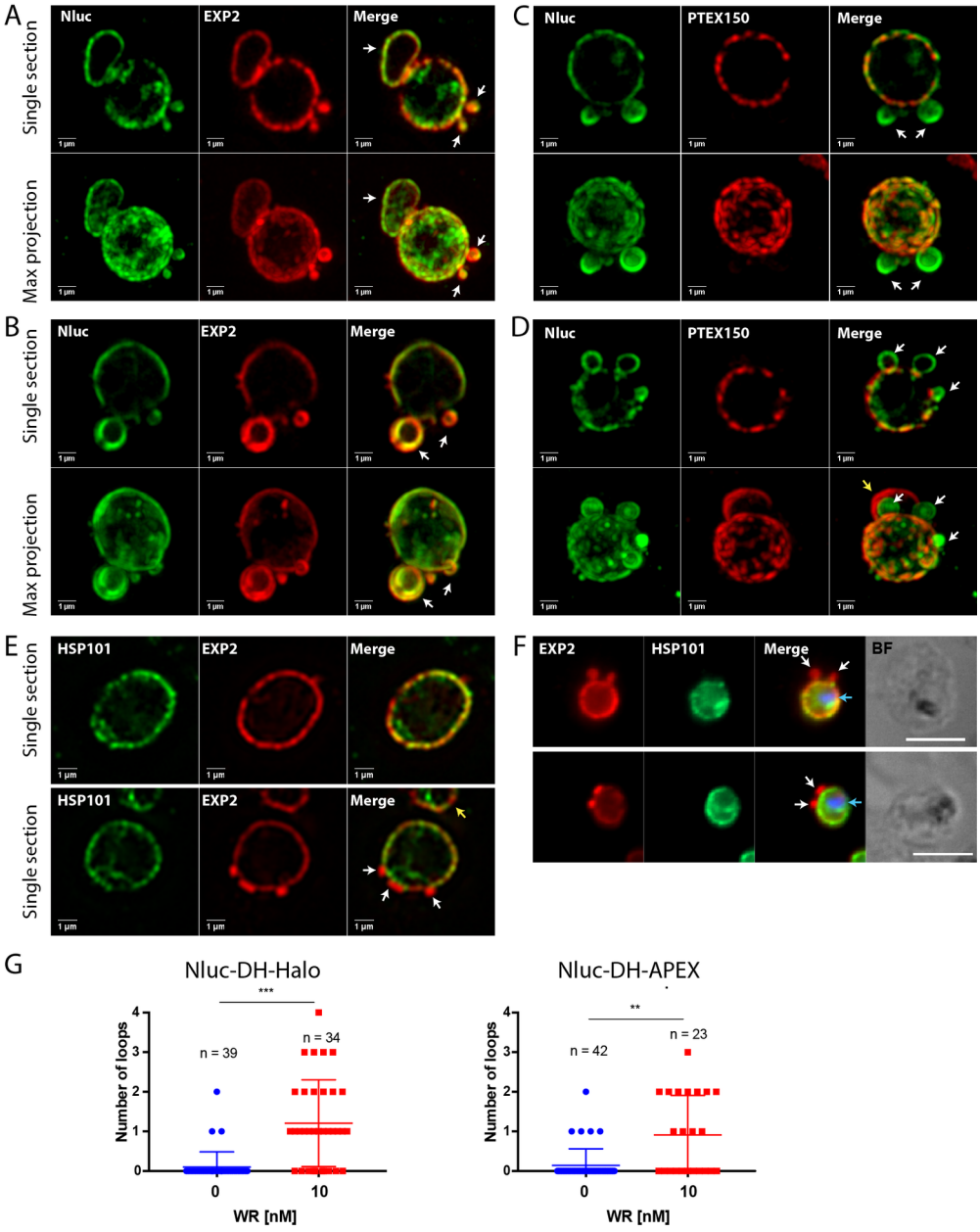

Fig 4.tif

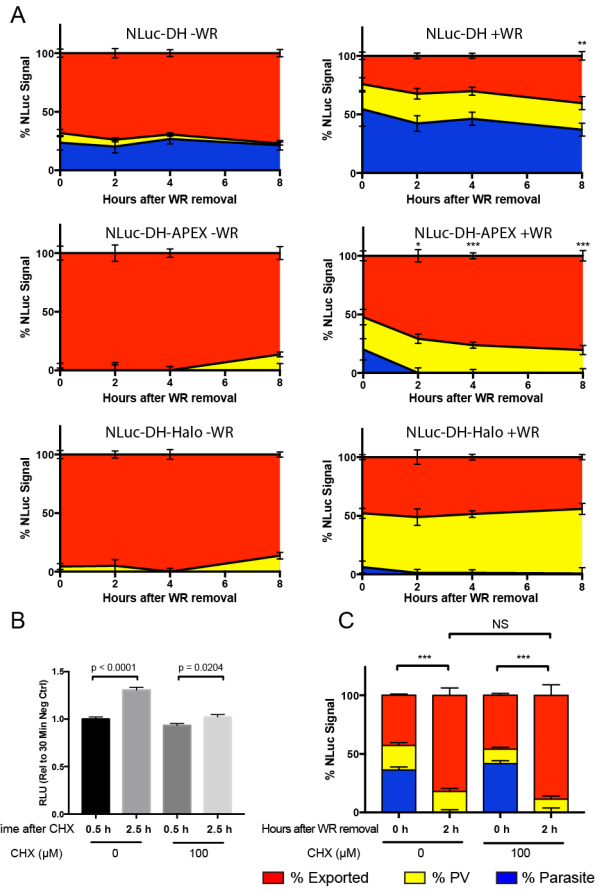

Fig 5.tif

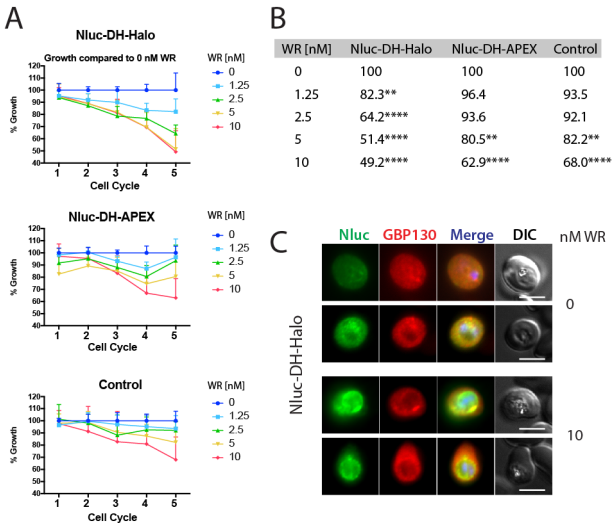

WR [nM]	Nluc-DH-Halo	Nluc-DH-APEX	Control
0	100	100	100
1.25	82.3**	96.4	93.5
2.5	64.2****	93.6	92.1
5	51.4****	80.5**	82.2**
10	49.2****	62.9****	68.0****

Fig 6.tif

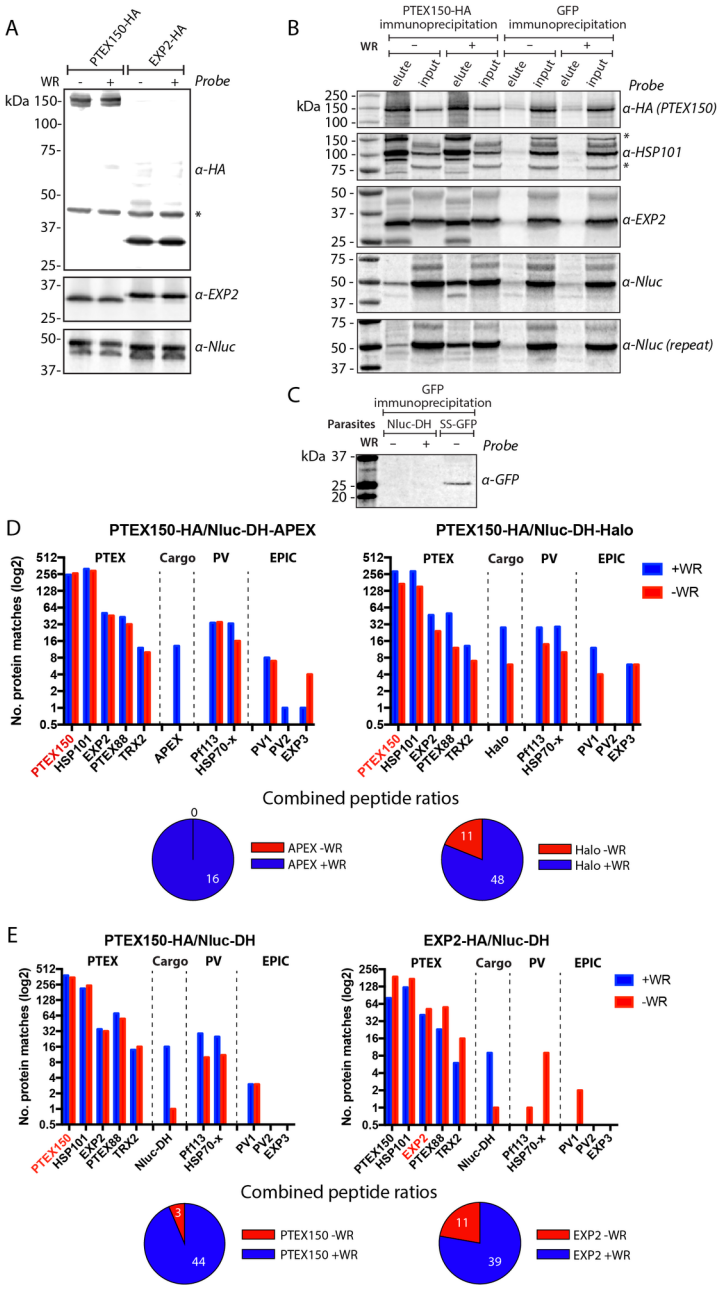

Fig 7.tif

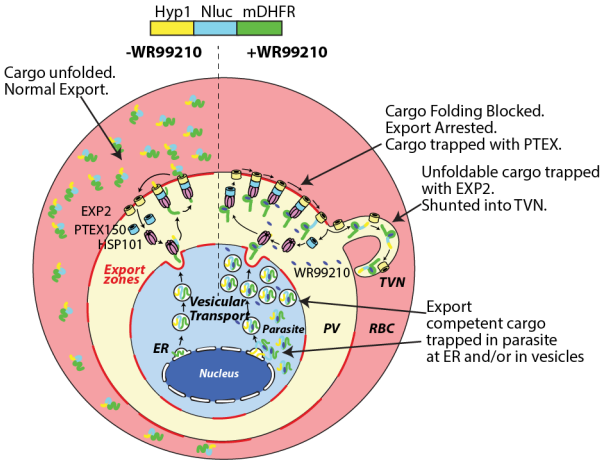

Fig 8.tif

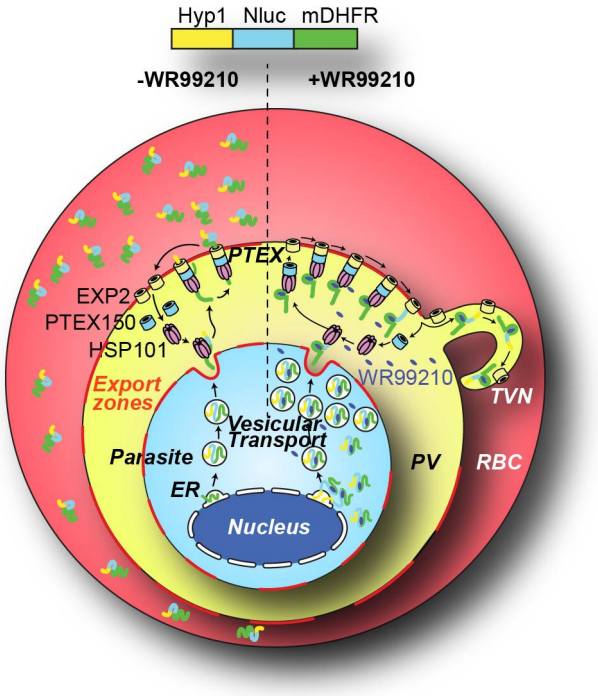

TRA_12577_AbstractFig.jpg